

# Hochschule Karlsruhe

University of Applied Sciences  
Faculty of Information Management and Media



Hochschule Karlsruhe  
Technik und Wirtschaft  
UNIVERSITY OF APPLIED SCIENCES

Bachelor Thesis

## **Macroalgal distribution shifts during the climate change induced glacier retreat in Potter Cove, West Antarctic Peninsula, 1993-2016**

Author:

**Lukas-Alexander Weber**

May 15, 2017

Advisors:

**Prof. Dr. habil. Mark Vetter**

Hochschule Karlsruhe

**Dr. Kerstin Jerosch**

Alfred-Wegener-Institut Bremerhaven

in collaboration with the

**Alfred Wegener Institute Bremerhaven  
Helmholtz Centre for Polar and Marine Research**



**ALFRED-WEGENER-INSTITUT**  
HELMHOLTZ-ZENTRUM FÜR POLAR-  
UND MEERESFORSCHUNG

## Abstract

The West Antarctic Peninsula is one of the fastest changing regions on earth due to global warming. Consequent retreat of Fourcade Glacier in Potter Cove (PC), King George Island, released 1.5 km<sup>2</sup> of newly ice-free water areas in the last 60 years. Macroalgae, important primary producers in the benthic Antarctic ecosystem, were evidenced to colonize some of these areas. To reconstruct the spatial process of this shift, macroalgal transect data sets, first recorded in 1993 and last in 2016, as well as environmental predictors are available owing to many years of field studies in PC. Species Distribution Models (SDMs) can statistically link species samples with raster predictors to project distribution maps. Macroalgal data is therefore prepared for modeling and grouped in three time steps, 1993-1996, 2008-2012 and 2016. Physical predictors for macroalgal distribution used in this thesis are: Probability of hard substrate occurrence, suspended particulate matter, bathymetry and slope. For each time step, SDMs are calculated for the species *H. grandifolius*, the grouped *Desmarestia* genus, remaining *Phaeophyceae* (brown algae) and *Rhodophyceae* (red algae). Community Maps, generated by classifying model results, are presented for the three time steps. They reveal information on species-richness and composition. Additionally a change raster is calculated for area gain and loss during a period between two time steps. In 1993-1996, 2.77 km<sup>2</sup> of the study area was populated by algae. This area increased by 1.38 km<sup>2</sup> to 4.15 km<sup>2</sup> in 2016. 2008-2012 results confirm this growth. 0.5 km<sup>2</sup> of this gain is located in areas, which were covered by glacier ice in 1956. Species of the class *Rhodophyceae* show as pioneers in exploring new habitable areas. Complexity and vertical distribution of macroalgal community is reduced in newly ice-free water areas near the glacier due to increased sediment input.

**Keywords:** Macroalgae, Habitat shift, Species Distribution Models, Community maps, Change detection, Glacier retreat, Potter Cove, Antarctic Peninsula

## **Declaration of Authorship**

I hereby certify that this thesis has been composed by me and is based on my own work, unless stated otherwise. No other person's work has been used without due acknowledgment in this thesis. All references and verbatim extracts have been quoted, and all sources of information, including graphs and data sets, have been specifically acknowledged.

---

Place, Date

---

Signature

# Table of Contents

<b>Abstract.....</b>	<b>I</b>
<b>Declaration of Authorship.....</b>	<b>II</b>
<b>Table of Contents .....</b>	<b>III</b>
<b>List of Figures.....</b>	<b>V</b>
<b>List of Tables .....</b>	<b>V</b>
<b>List of Abbreviations .....</b>	<b>VI</b>
<b>1 Introduction .....</b>	<b>1</b>
<b>2 Background .....</b>	<b>3</b>
2.1 Macroalgae .....	3
2.2 Species distribution models.....	7
2.3 Change detection .....	10
<b>3 Data and Methods.....</b>	<b>11</b>
3.1 Study area.....	11
3.2 Data .....	13
3.2.1 Macroalgal data.....	13
3.2.2 Additional data.....	14
3.3 Preparation of macroalgal data for modeling.....	14
3.3.1 1993/1994 Klöser et al. data .....	14
3.3.2 1994-1996 Quartino and Boraso de Zaixso data .....	15
3.3.3 2016 Jerosch data.....	16
3.3.4 Grouping and merging macroalgal data into time steps .....	19
3.4 Modeling .....	19
3.5 Community mapping.....	20
3.6 Change detection .....	21
3.7 Glacier retreat and newly ice-free water areas .....	21
<b>4 Results and Discussion .....</b>	<b>23</b>
4.1 Model results .....	23
4.1.1 1993-1996 .....	25
4.1.2 2008-2012 .....	25
4.1.3 2016 .....	25
4.2 Community maps .....	27
4.3 Changes in macroalgal population of PC.....	28

---

4.4	Development of ice-covered water areas in PC in combination with macroalgal distribution shifts .....	31
4.5	Future monitoring of macroalgae in PC .....	33
<b>5</b>	<b>Conclusion .....</b>	<b>34</b>
	<b>References .....</b>	<b>36</b>
	<b>Appendix 1: Input species data sets .....</b>	<b>40</b>
	<b>Appendix 2: Model results .....</b>	<b>41</b>
	<b>Appendix 3: Response curves .....</b>	<b>42</b>
	<b>Appendix 4: Community maps .....</b>	<b>44</b>

## List of Figures

Figure 1: Taxonomy of the three dominant macroalgal species at WAP .....	4
Figure 2: Vertical distribution of macroalgae compared to wavelengths of light penetration in summer.....	5
Figure 3: Seabed cover in PC according to Klöser et al. (1996) .....	6
Figure 4: Common macroalgae in PC.....	6
Figure 5: Species distribution modeling process .....	9
Figure 6: Community modeling with single species models.....	10
Figure 7: Post-classification comparison in form of a change matrix .....	10
Figure 8: Location of the study area from small- to large scale .....	12
Figure 9: Coverage analysis combined with a georeferenced transect.....	15
Figure 10: Relocated biomass samples along depth contours based on the original attribute table.....	15
Figure 11: Interpolation of multiple points with constant gaps .....	17
Figure 12: Workflow of combining video analysis tables with GPS files.....	18
Figure 13: Analyzed video transects combined with GPS positions .....	18
Figure 14: Workflow of processing a downloaded Landsat 8 scene .....	22
Figure 15: Overlapping model results of the respective time steps.....	23
Figure 16: Response curves from both best single models and ensemble model....	24
Figure 17: TSS evaluation scores of final models used in the following analyses..	24
Figure 18: Ensemble model of 2016 Rhodophyceae class .....	26
Figure 19: Community maps of the three time steps.....	27
Figure 20: Small scale comparison of community maps in different time steps....	28
Figure 21: Change detection between the periods ~1993-2010 and ~2010-2016 ...	29
Figure 22: Area populated by macroalgae [km <sup>2</sup> ].....	30
Figure 23: New ice-free water areas in PC due to glacier retreat. ....	31
Figure 24: New ice-free water areas in PC compared with macroalgal population of 1996 and 2016.....	32

## List of Tables

Table 1: Available species data in PC .....	13
Table 2: Recording days, time format of used GPS recorder and analyzer of the result videos. ....	16
Table 3: Extract of the GPS shapefile attribute table (18.01.2017).....	16
Table 4: Extract of the Microsoft Excel video analysis table (18.01.2017) .....	17
Table 5: Grouping macroalgal transects into time steps for modeling.....	19
Table 6: Community classification of a time step based on macroalgal modeling results .....	21
Table 7: Quantity of used BIOMOD modeling approaches .....	24

## List of Abbreviations

ANN	Artificial neural network
AUC	Area under the relative operating characteristic curve
AWI	Alfred Wegener Institut
CTA	Classification Tree Analysis
FDA	Flexible Discriminant Analysis
GAM	Generalized Additive Models
GBM	Generalized Boosted Models
GIS	Geographic information systems
GLM	Generalized Linear Models
IAA	Instituto Antartico Argentino
KGI	King George Island
MARS	Multivariate adaptive regression splines
MaxEnt	Maximum Entropy Modeling
PAR	Photosynthetically active radiation
PC	Potter Cove
RF	Random Forest
SDMs	Species distribution models
SPM	Suspended particulate matter
SRE	Species Range Envelope
TOV	Towed operated vehicle
TSS	True Skill Statistic
USGS	United States Geological Survey
WA	Weighted Average
WAP	West Antarctic Peninsula

# 1 Introduction

The West Antarctic Peninsula (WAP) is one of the fastest changing regions on earth due to global warming (Vaughan et al. 2003). This leads to retreating glacier fronts (Cook et al. 2005) and significant changes of marine ecosystems (Clarke et al. 2007; Brey et al. 2011; Sahade et al. 2015). Potter Cove (PC), a small cove of King George Island (KGI), is located at the South Shetland Islands at the northern top of WAP. The recent front of PC's Fourcade Glacier has shifted more than one kilometer towards the coastline within 60 years (Rückamp et al. 2011), releasing water areas in the cove from ice. Therefore these areas became suitable for benthic colonization and photosynthesis mainly due to light availability. Quartino et al. (2013) showed that some of these newly ice-free areas are settled by macroalgae which are a crucial part of the Antarctic coastal ecosystem. These important benthic primary producers provide habitat and food for grazers like amphipods, sea stars or fishes (Huang et al. 2007; Iken et al. 2009; Wiencke and Amsler 2012). Shifts in macroalgal distribution will probably lead to a shift of adapted species (Iken et al. 2009), thus monitoring those changes is environmentally important.

No long-ranging comparable monitoring of macroalgal distribution is realized in PC yet. However an adaptation is necessary for better insight in ecosystem changes within PC and additionally for predicting changes in slower warming regions of Antarctica. The aim of this study is to reconstruct macroalgal distribution shifts in PC from past to present and to associate them with occurred glacier retreat. Further the utility of used methods is discussed to provide a continuous monitoring in future.

The scientific Carlini (former Jubany) Base at PC enabled comprehensive interdisciplinary long-term field studies such as photo/video-transects along depth gradients within PC. Six transect data sets are available, first recorded in 1993 and last in 2016. Analyzing those transects give among others indication for occurring macroalgal species (Klöser et al. 1996; Quartino and Boraso de Zaixso 2008; Quartino et al. 2013; Sahade et al. 2015; Jerosch et al. n.d.). Additionally, species distribution maps may be derived from this data (Jerosch et al. n.d.). As an approach for monitoring macroalgal distribution shifts, community maps are created from available transects using species distribution models (SDMs). Actual and past distributions will be predicted and based on the results, shifts in macroalgal distribution will be mapped using change detection methods.

The main focus thereby is to prepare historical macroalgal data for species distribution modeling and to compare the results with newer data. SDMs have proven to be valuable for mapping macroalgal distribution (Jerosch et al. n.d.). Therefore other approaches for monitoring are not taken into account. For environmental terms probable shifts are associated with glacier retreat in PC. A transfer of the results to other parts of Antarctica are not part of this thesis but could be subject of prospective studies.



---

The following Chapter 2, Background, gives a theoretical introduction into macroalgae in Antarctica and the process of species distribution modelling, as well as into the operating principle of change detection. Chapter 3, Data and Methods, presents the study area and the available data. Methods applied in this thesis to achieve desired results are described in detail. Chapter 4 submits the results and discusses their quality and meaning. An outlook on future modelling of macroalgae is given at the end of this Chapter. Chapter 5 concludes this thesis by answering its central research questions.

## 2 Background

### 2.1 Macroalgae

Macroalgae, also known as seaweeds, are generally widespread across the globe. A significant increase of their biomass at cultivated coastlines is induced by eutrophication, displacing other native inhabitants (Morand and Briand 1996). In Antarctica, where direct human encroachments on ecosystems are low, natural reaction of macroalgae to global warming may be observed without human pollution (Halpern et al. 2008).

Macroalgae at the WAP are adapted to the prevalent extreme climate. 35%, with increasing tendency, are endemic. Most species are shade adapted to survive darkness in winter caused by short days and ice cover. They have a low light demand for photosynthesis and most species are season anticipators, starting to grow in winter. In spring/summer, when ice breaks and days are getting longer, light penetrates deep into the water and algae are able to intensify their growth and to create more biomass (Wiencke and Amsler 2012). As a consequence, seaweed biomass is subject to a strong seasonal variability. A further challenge for seaweeds is to withstand damaging UV radiations during that time of season, leading to a higher UV tolerance of species distributed in shallow waters compared to algae occurring in deeper vertical ranges (Gomez and Huovinen 2015). Additionally spores of algae living in the intertidal and sublittoral zone and procreating in spring were shown to be UV tolerant (Zacher et al. 2009).

Erosion and decomposition of plants as well as detached macroalgae by storms or water movements provide nutrients for the ecosystem (Brouwer 1996). Fishes and invertebrates find food and shelter in seaweed habitats and are often specialized for a specific macroalgal species (Iken et al. 2009). Macroalgae are thereby the habitat forming life form in stony shores with important roles for the community's food chain.

Primarily occurring macroalgae classes at WAP are *Phaeophyceae* (brown algae) and *Rhodophyceae* (red algae). They are the dominant component of the sublittoral (from low tide to the edge of continental shelf) ecosystem on a rocky seafloor (hard substrate). Big brown algae of the order *Desmarestiales* (*Desmarestia anceps*, *Desmarestia menziesii* and *Himantothallus grandifolius*) contribute to most of macroalgal biomass (Brouwer 1996; Quartino and Boraso de Zaixso 2008). Their taxonomy is visualized in Figure 1. The pattern of their vertical distribution is simplified *D. menziesii* in the upper sublittoral zone, followed by *D. anceps* to a depth up to 20-30 meters and in deeper areas, when *Desmarestia* vanishes, *Himantothallus grandifolius*. The big *Desmarestiales* are mostly neighboring smaller *Phaeophyceae* and *Rhodophyceae* species.

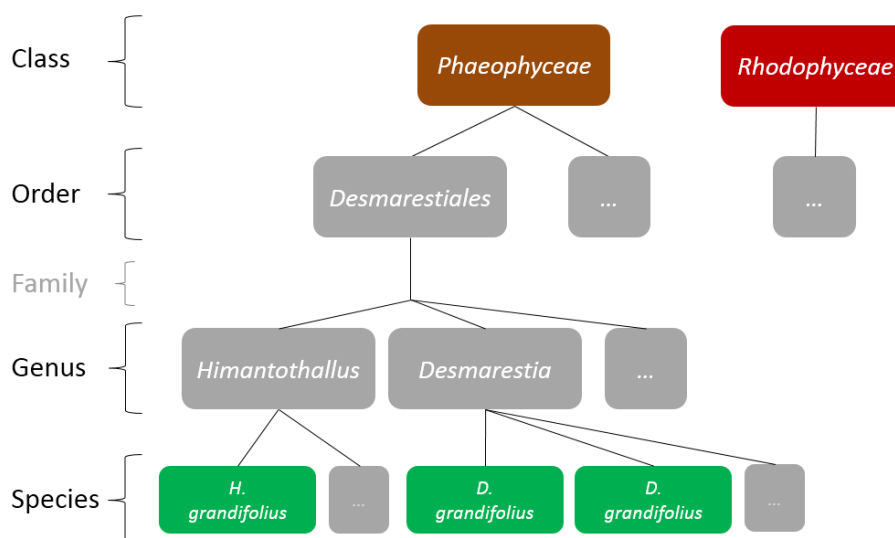


Figure 1: Taxonomy of the three dominant macroalgal species at WAP (green), starting from the two primarily occurring macroalgae classes *Phaeophyceae* (brown algae) and *Rhodophyceae* (red algae). The classification of “Family” is not captured in this work and thus skipped to simplify the figure. Information on taxonomy was collected from the World Register of Marine Species (WoRMS) and gained by personal communication with K. Zacher (AWI) and C. Neder (Universidad Nacional de Córdoba, UNC).

Usually borders between macroalgal zones are fluent and there is a coexistence between the species (Wiencke and Amsler 2012; Gomez and Huovinen 2015). The described vertical distribution is applicable to the area between Signy Island and Anvers Island (see Figure 8b). Nevertheless, macroalgal species diversity and biomass decrease from north to south due to the increase of ice coverage and reduced light availability. Through rising temperatures at WAP and consequential decline of sea ice cover, Wiencke and Amsler (2012) predict a southwards shift of macroalgae distribution.

The distribution of macroalgae at KGI is well studied. Gomez and Huovinen (2015) compared the vertical occurrence of four common species at KGI with wavelength of light penetration (Figure 2). As the fourth biggest supplier of biomass within *Phaeophyceae* (Quartino and Boraso de Zaixso 2008), *Ascoseira mirabilis* is added to the previously introduced species. This species is well adapted to high UV exposure in spring/summer, while deeper residing species like *Himantothallus grandifolius* have fewer UV tolerance. Photosynthetically active radiation (PAR), which organisms use for photosynthesis, reaches up to a depth of approximately 30 meters, restricting a deeper colonization of coastal regions’ seabed (Gomez and Huovinen 2015).

In PC the increase of turbidity in seasons of strong light penetration and resulting melt water lead to a shift in maximal depth distribution of macroalgae. In areas with high sediment input at the southern coast and around the glacier, vertical distribution is reduced. That explains why areas exposed to glacier retreat and recent ice melting areas are populated by seaweed, but not in a comparative depth like in clear water. A beneficial effect of turbidity is a decreasing exposure to UV radiation (Deregibus et al. 2015).

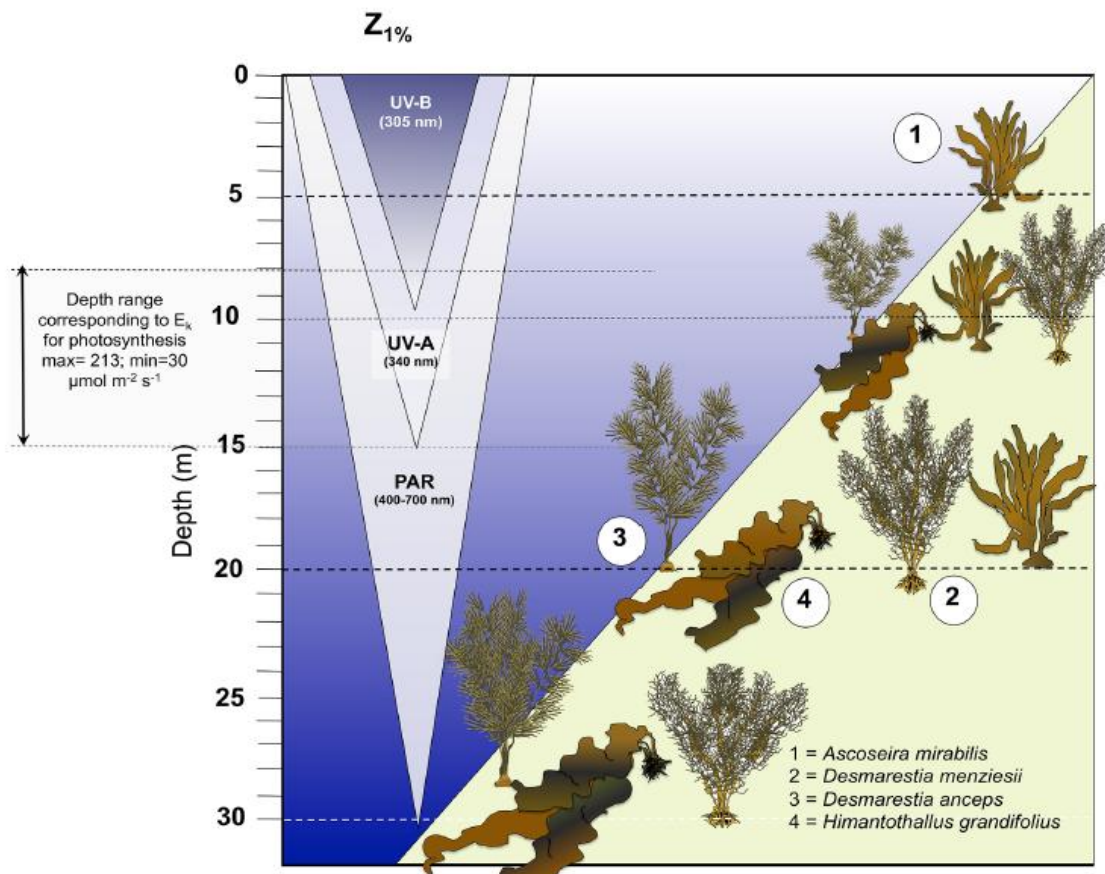


Figure 2: Vertical distribution of macroalgae compared to wavelengths of light penetration in summer. UV-B and UV-A have short wavelengths and are therefore harmful for macroalgae causing DNA-damage (Gomez and Huovinen 2015).

Quartino and Boraso de Zaixso (2007) published biomass and production data of macroalgae in PC showing that *Desmarestia anceps*, *D. menziesii*, and *Himantothallus grandifolius* represent 80% of local biomass. Smaller species with a frequent prevalence of 25% or higher are relevant for a general view, such as *Iridaea cordata*, *Curdiea racovitzae*, *Plocamium cartilagineum* (Rhodophyceae) and *Ascoseira mirabilis* (Phaeophyceae).

The distribution of macroalgae along depth gradients in PC is described by Klöser et al. (1996) and Marcías et al. (2017) as follows:

- Intertidal zone: Avoided by large algae, populated mostly by small red algae species (*Pyropia endiviifolia* in the highest level, other species like *Iridaea cordata* and *Palmaria decipiens* following).
- Upper sublittoral: *D. menziesii* in steep areas which are not exposed to much water movement, *Palmaria decipiens* and *Ascoseira mirabilis* in flat areas with regular movement.
- Central sublittoral: *D. anceps* dominates on hard substrate while *H. grandifolius* may occur on loose material.
- Deep sublittoral: *H. grandifolius* dominates.

This pattern is illustrated in Figure 3.

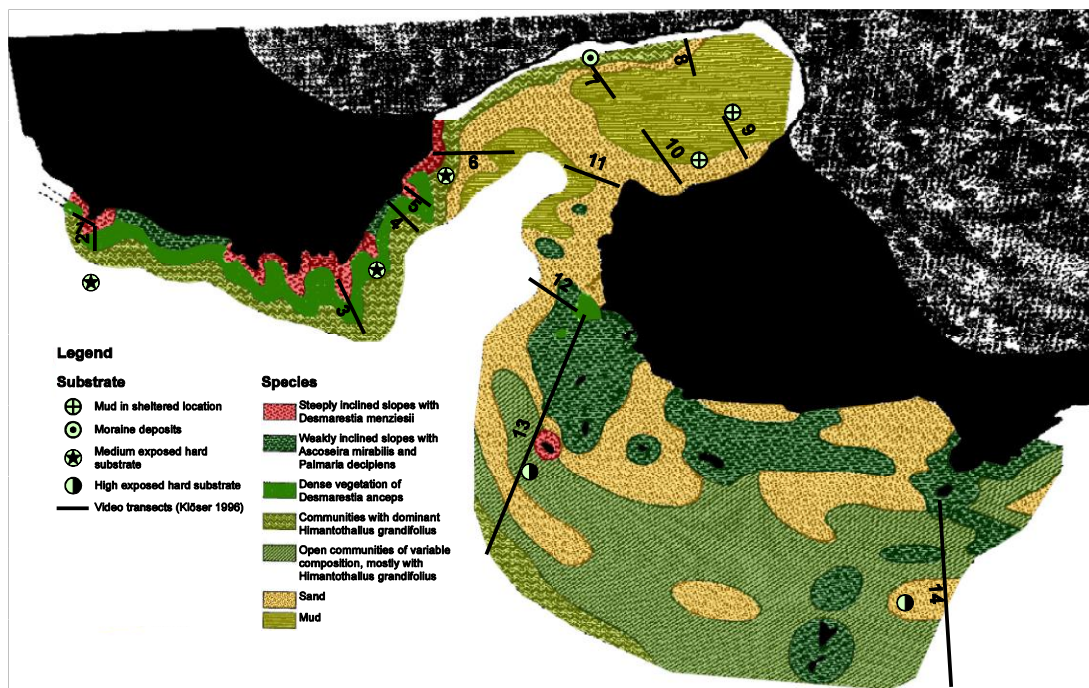


Figure 3: Seabed cover in PC according to Klöser et al. (1996), derived from visualized video transects. Substrate samples taken over from Klöser and Arntz (1995). Original figures were georeferenced and digitalized (see Chapter 3.3.1).

An assortment of introduced seaweeds is visualized in Figure 4.

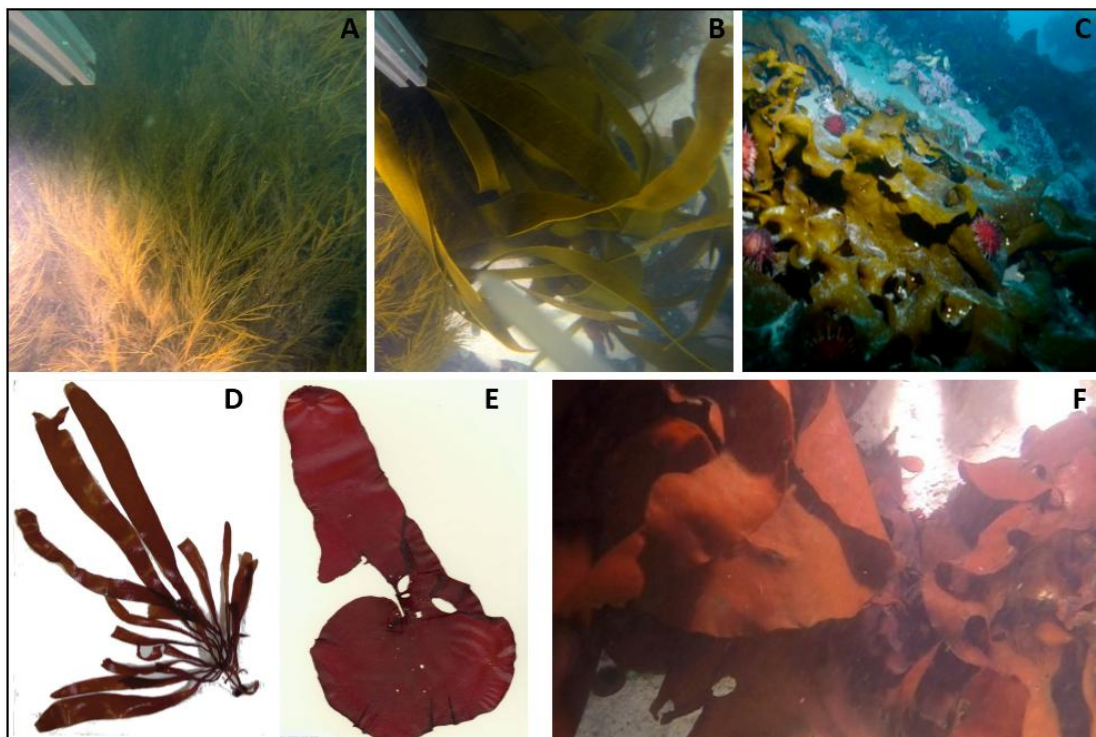


Figure 4: Common macroalgae in PC. Upper row: *Phaeophyceae*; lower row: *Rhodophyceae*. **A** *Desmarestia* genus (species are hard to distinguish (Zacher pers. comm.)) **B** *Ascoseira mirabilis* **C** *Himantothallus grandifolius* **D** *Palmaria decipiens* **E** *Iridaea cordata* **F** *Rhodophyceae* (probably *I. cordata* (Zacher pers. comm.))

Sources: **A, B, F**: Stills of videos collected by K. Jerosch **C**: Report on Gomez and Huovinen (2015): <http://www.conicyt.cl/pia/2015/08/13/macroalgas-antarticas-respon-den-al-estres-luminico/> downloaded on 09.03.2017 **D**: Published in Becker et al. (2011) **E**: Collected by Fredericq and Ramirez (1994): [http://ucjeps.berkeley.edu/new\\_images/MHH\\_iridaea.jpg](http://ucjeps.berkeley.edu/new_images/MHH_iridaea.jpg) downloaded on 09.03.2017



## 2.2 Species distribution models

SDMs are statistical methods to link scattered biological data with mapped environmental predictor variables (Ferrier et al. 2002). During the last two decades utilization of SDMs increased significantly within a broad range of applications. They can, among others, generate habitat suitability maps or quantify habitat conditions under which a species is able to live or not (environmental niche). Additionally, results received from SDMs may be projected into future or past scenarios. This information is valuable for conservation management or for testing the impact of environmental changes (Guisan and Thuiller 2005; Thuiller et al. 2009).

Several steps are required to build a habitat suitability map with a SDM (Hijmans and Elith 2017):

- (1) Collecting geographic locations of species' occurrence or optional absence.
- (2) Choosing and processing environmental predictor parameters influencing the species.
- (3) Building a statistical model with the association between species and predictors.
- (4) Projecting the species distribution in the area of interest by using model results.

Presence or absence data (1) originates from multiple sources. It can costly be collected systematically, can be reused from previous studies or can come from museum databases. Especially when presence-only data is used, pseudo absences or background data should be sampled. A sufficient amount of well spread species data is crucial for model applicability (Guisan and Thuiller 2005; Barbet-Massin et al. 2012).

Parameters chosen for the prediction of species distribution (2) should reflect environmental influences concerning the conditions where it is able to live or not. These influences include regulators, disturbances and resources (Guisan and Thuiller 2005). Transferred on the introduced macroalgae, depth would be considered a regulator, turbidity through SPM a disturbance. Environmental predictors are mostly obtained by remotely sensed or interpolated raster data and prepared in geographic information systems (GIS) (Ferrier et al. 2002). Detecting correlations between parameters is important, especially if the model is intended to explain the driving forces or to be extrapolated in time. If this work is not done, received information on the environmental niche of a species may be misinterpreted (Dormann et al. 2012). Choosing relevant predictors will improve the quality of the model result, thus biological knowledge of the modeled species is of advantage (Elith and Leathwick 2009). To model future or past scenarios, one or more parameters are replaced by predicted values (received e.g. from climate models) and compared with the original results (Thuiller et al. 2009).

Model building (3) includes choosing, fitting and evaluating a model (Hijmans and Elith 2017). A wide range of SDMs is implemented, complicating ecologists' decision about which model is most suitable for their study (Elith and Graham 2009). One approach is to test multiple algorithms and to choose the best performing ones, based on model evaluations. Model fitting is based on the used model technique. Commonly used are regression (e.g. Generalized Linear Models -GLM-, Generalized Additive Models -GAM-), machine learning (e.g. Random Forest -RF-, Maximum Entropy Modeling -MaxEnt-) and classification (e.g. Classification Tree Analysis -CTA-) methods (Thuiller et al. 2009). The known species locations and the predictor values at these sites are used to calculate the influence of single parameters on the species. Most models compile a formula which describes the species' occurrence using additive combinations of predictors (Elith and Leathwick 2009; Hijmans and Elith 2017). Usually these models are trained with only a part of species data, saving remaining testing data for cross validation. Various model evaluation techniques are established, including area under the relative operating characteristic curve (AUC) and true skill statistic (TSS). These methods can validate model accuracy (Thuiller et al. 2009; Hijmans and Elith 2017). The accuracy of models depends on the biotic and algorithmic methodology (Marmion et al. 2009).

In order to project the model into an area of interest (4), the statistical model is used to predict where a species might live. There are two types of predictions, namely interpolation and extrapolation. The area, where model training samples are located, may be mapped by model-based interpolation to unsampled sites. Alternatively, the model may be extrapolated to either another place, when the same environmental parameters are available, or to future/past scenarios. For example, a model trained in PC could interpolate presence probability in the particular inlet. Furthermore, it could also predict the distribution in the neighboring Marian cove (extrapolation). However, the latter has to be handled carefully due to increased susceptibility error and transferability problems (Elith and Leathwick 2009). To eliminate uncertainties, sometimes more than one projection is calculated using different model runs or different model techniques. Mean or weighted average (WA) are the best approaches for combining those single models into an ensemble model. WA uses elevation scores to give more weight to better performing models (Marmion et al. 2009).

Figure 5 visualizes the process of making a habitat suitability map.

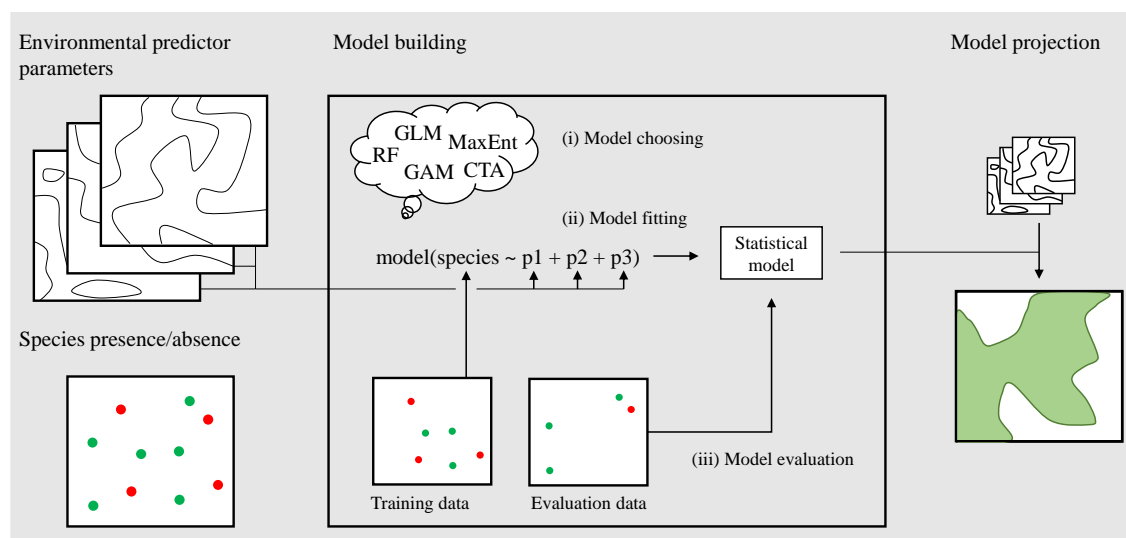


Figure 5: Species distribution modeling process. Species data is split into training and evaluation data. After choosing a model (i) it is fitted by compiling a formula with species data as dependent and environmental predictor data as independent variables (ii) (formula from Hijmans and Elith 2017). The result is a statistical model, which may be cross-validated with evaluation data (iii). Subsequently, it may be projected by applying the model for every pixel where environmental parameters are available.

Since co-occurring species may have intersecting niches, overlapping results of single SDMs may provide information about species-richness and composition of an ecosystem (Araújo and Guisan 2006; Pineda and Lobo 2009). The four previously presented steps are extended by a fifth (Cawsey et al. 2002):

#### (5) Community mapping

Community composition mapping links species distribution modeling with traditional ecological mapping. An example for traditional mapping is the seabed cover map in Figure 3. A composition map may be realized by merging single species model results with numerical classification. There are two basic ways to do that: “classification-then-modeling” and “modeling-then-classification”. As the names indicate, both methods differ primarily in order of processing. Classification in this case is usually based on cluster analysis (Lenihan 1993; Ferrier et al. 2002). Figure 6 extends Figure 5 with a “modeling-then-classification” community mapping, while detailed model building is simplified.



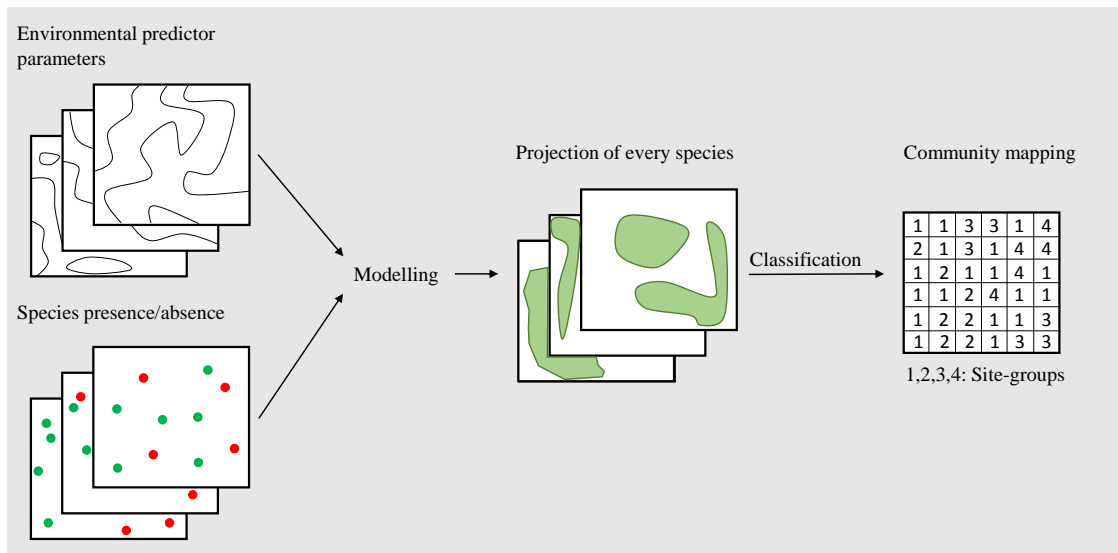


Figure 6: Community modeling with single species models. Presence/absence data of multiple species are used to project the single models. These projections are classified to obtain site-groups which have similar species compositions.

### 2.3 Change detection

Change detection is a common field primarily used in Remote Sensing, but is also deployed in underwater sensing. It may be applied on data sets which are located in the same area but originate from different times. Receiving regions of change over the course of time is required in multiple scientific fields, including biogeography. Multiple techniques are available for detecting and mapping ecosystem changes (Lu et al. 2004; Coppin et al. 2004; Radke et al. 2005).

When working with multitemporal classified raster data, an obvious method is the comparative analysis of each pixel value in time one ( $t_1$ ) and time two ( $t_2$ ), called post-classification comparison. It is worth mentioning that the accuracy of this method depends on the previous classification quality (Mas 1999). Comparison of area coverage may hint information on area loss or gain within a certain class. More explicit is cross tabulation of all available classes which contain “from-to” information from a particular class to another (Alphan et al. 2009). Such a matrix and its sources are exemplary visualized in Figure 7.

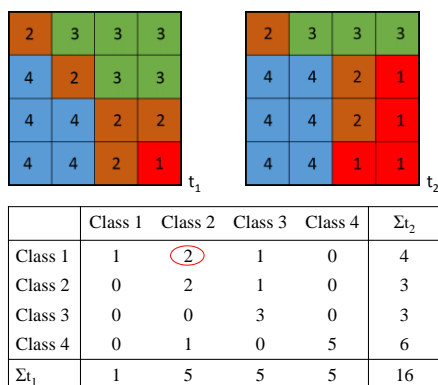


Figure 7: Post-classification comparison in form of a change matrix. Two classified rasters  $t_1$  and  $t_2$  are compared based on their pixel values. The main diagonal describes the quantity of pixels with no change. Other entries reveal the pixels of area gain in the rows and area loss in the columns. The marked 2 reveals that class 1 gained two pixels from class 2, vice versa class 2 lost two pixels to class 1.

## 3 Data and Methods

Available transect analysis data of macroalgae in PC is prepared and separated in suggestive time steps with sufficient samples for species distribution modeling at most detailed level of their taxonomy. Single species model results are used for creating a community composition map in the respective time step. A post-classification change detection analysis is applied on the multitemporal results, using the composition maps as “classified” data sets. The results are evaluated and compared with newly ice-free areas in PC in order to recognize an adaption pattern of macroalgae.

### 3.1 Study area

PC (62°14'S, 58°41'W) is an inlet at the south of KGI, flanked by the ice-free Potter and Barton Peninsula and determined by Fourcade Glacier in the north. KGI is the biggest and thus one of the major islands of the 540 km long South Shetland Islands chain at the WAP (Figure 8) (Klöser et al. 1993; Rückamp et al. 2011).

In 1985 the Alfred Wegener Institut (AWI) and the Instituto Antartico Argentino (IAA) initiated a research cooperation resulting in a collaborative use of the Argentine Carlini (former Jubany) Base at PC, beginning in 1991 (Wiencke et al. 1998).

Klöser et al. (1994 and 1995) described the topography and hydrography of PC as follows:

The cove is separated into an inner and an outer part bounded by the first glacier moraine examined closely by Wölfl et al. (2016) and visualized in Figure 1. The inner part is up to 50 meters deep while the outer cove may reach a depth of 200 meters. The northern and eastern parts of the inner cove are restricted by pending 50 meters high glacier cliffs. To the south, where the research station is located, the cove passes into a coarsely sanded beach. Icebergs, drifting into the cove through occurring currents, as well as aborting glacier ice run ashore on a flat platform at the southern coast, creating seabed damages by ice scouring (Philipp et al. 2011). Melt water during summer season reduces the salinity of the cove and carries a significant amount of suspended sediments (suspended particulate matter (SPM)) into the cove (Schloss et al. 2012), causing differently colored water and the effect of different absorption gradients of light radiation. Melting water enters both through the glacier itself and through melt water creeks at the southern shore of the cove, thus turbidity is maximum in this part. The outer cove coast at Barton Peninsula is usually unaffected by this turbidity.

Other seasonal variations at PC are the day length, which varies between 20 hours in summer and 5 hours in winter, as well as pack ice covering parts of the cove (at least 15%) averaged 233 days a year, from April to November. Mean air temperature differs between -6.3 °C in July and +2.5°C in January, while water temperature varies between

about  $-2\text{ }^{\circ}\text{C}$  and  $+1.5\text{ }^{\circ}\text{C}$  (Wiencke and Amsler 2012; Schloss et al. 2012). The area is subject to a maritime climate causing glaciers to be sensitive to climate change. During the past 50 years temperatures at WAP raised up to  $3\text{ }^{\circ}\text{C}$ . Glaciers on KGI experienced retreat and surface lowering, resulting in an ice cover loss of up to one kilometer at PC in the same time (Schofield et al. 2010; Brey et al. 2011; Rückamp et al. 2011).

Thus, biological impacts of those changes on the WAP are an important field of study, providing a chance to predict reactions of ecosystems in other parts of Antarctica, which probably experience further warming (Schofield et al. 2010). Adaptions of benthic ecosystems at KGI were analyzed in various studies (Brey et al. 2011; Schloss et al. 2012; Deregibus et al. 2015; Sahade et al. 2015; Torre et al. 2017; Jerosch et al. n.d.).

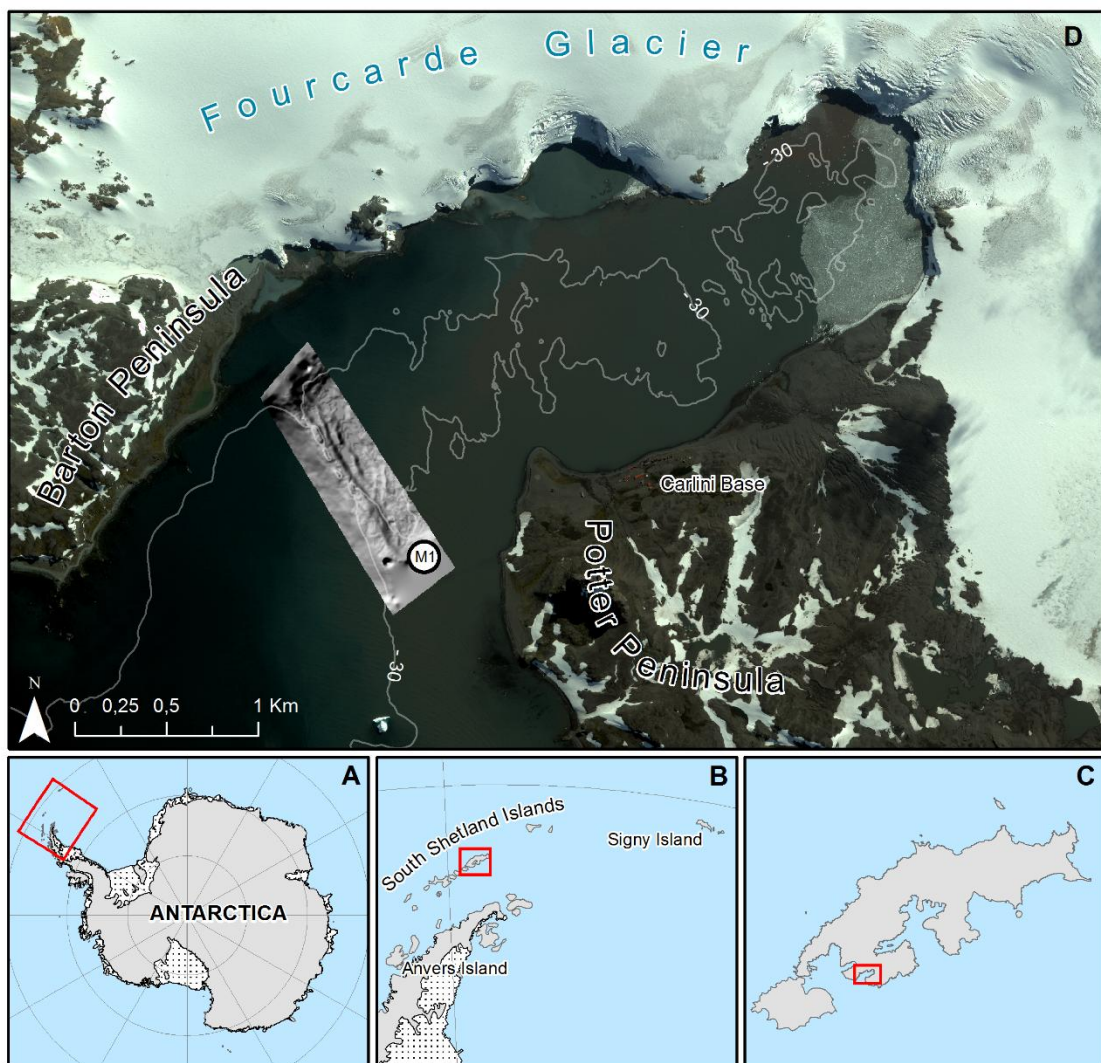


Figure 8: Location of the study area from small- to large scale: **A** The continent Antarctica **B** The northern tip of WAP, showing Signy and Anvers Island as limiter of macroalgal distribution **C** KGI, the biggest of the South Shetland Islands with **D** the inlet PC visualized by a pansharpened WorldView2 satellite image of 2013 (DigitalGlobe 2014). M1 shows the hillshade of the moraine complex separating inner (northwest) and outer (southeast) cove according to Wölfl et al. (2016). Data made available by: AWI

## 3.2 Data

### 3.2.1 Macroalgal data

As introduced, many photo/video-transects of macroalgae have been recorded in PC between 1993 and 2016. Table 1 gives an overview of which species data are available for which years. Taxonomy classes are sorted by their importance as presented in Chapter 2.2.

Table 1: Available species data in PC. *X* indicates that the column taxonomy is available but lacking detail. – indicates that the column taxonomy is not available. The Phaeophyceae column excludes *Desmarestia* and *H. grandifolius*.

	<i>Desmarestia</i>	<i>H. grandifolius</i>	<i>Phaeophyceae</i>	<i>Rhodophyceae</i>
<b>Klöser et al.</b> (data: 1993/1994, published: 1996)	<i>D. anceps</i> ; <i>D. antarctica</i> ; <i>D. menziesii</i>	<i>X</i>	<i>Ascoseira mirabilis</i> ; <i>Cystophaera jacquinotii</i>	<i>Ballia callitricha</i> ; <i>Gigartina skottsbergii</i> ; <i>Palmaria decipiens</i> ; <i>Pantoneura plocamioides</i> ; <i>Plocamium cartilagineum</i> ; <i>Sarcothalia papillosa</i>
<b>Quartino and Boraso de Zaixso</b> (data: 1994-1996, published: 2008)	<i>D. anceps</i> ; <i>D. antarctica</i> ; <i>D. menziesii</i>	<i>X</i>	<i>Adenocystis utriculari</i> ; <i>Ascoseira mirabilis</i> ; <i>Cystophaera jacquinotii</i> ; <i>Geminocarpus geminatus</i> ; <i>Halopteris obovata</i> ; <i>Petalonia fascia</i> ; <i>Phaeurus antarcticus</i>	<i>Ballia callitricha</i> ; <i>Callophyllis atrosanguinea</i> ; <i>Corallinaceae</i> ; <i>Curdiea racovitzae</i> ; <i>Delesseria lancifolia</i> ; <i>Georgiella confluens</i> ; <i>Gigartina skottsbergii</i> ; <i>Gymnogongrus antarcticus</i> ; <i>Gymnogongrus turquetii</i> ; <i>Hymenocladopsis crustigena</i> ; <i>Iridaea cordata</i> ; <i>Kallymenia antarctica</i> ; <i>Myriogramme smithii</i> ; <i>Nereoginkgo adiantifolia</i> ; <i>Neuroglossum ligulatum</i> ; <i>Notophycus fimbriatus</i> ; <i>Pachymenia orbicularis</i> ; <i>Palmaria decipiens</i> ; <i>Pantoneura plocamioides</i> ; <i>Phycodrya austrogeorgica</i> ; <i>Picconiella plumose</i> ; <i>Plocamium cartilagineum</i> ; <i>Porphyra endiviifolium</i> ; <i>Porphyra plocamiestrus</i> ; <i>Sarcodia montagnana</i>
<b>Quartino et al.</b> (data: 2008; published: 2013)	<i>D. anceps</i> ; <i>D. antarctica</i> ; <i>D. menziesii</i>	<i>X</i>	<i>Adenocystis utriculari</i> ; <i>Ascoseira mirabilis</i> ; <i>Phaeurus antarcticus</i>	<i>Ballia callitricha</i> ; <i>Corallinaceae</i> ; <i>Curdiea racovitzae</i> ; <i>Gigartina skottsbergii</i> ; <i>Hymenocladopsis crustigena</i> ; <i>Iridaea cordata</i> ; <i>Kallymenia Antarctica</i> ; <i>Myriogramme spp</i> ; <i>Neuroglossum ligulatum</i> ; <i>Palmaria decipiens</i> ; <i>Plocamium cartilagineum</i>
<b>Sahade et al.</b> (data: 2009; published: 2015)	<i>X</i>	<i>X</i>	<i>X</i>	<i>X</i>
<b>Wölfel</b> (data: 2011/Jan 2012, analysed by Quartino/Scharf; unpublished)	<i>D. anceps</i> ; <i>D. antarctica</i> ; <i>D. menziesii</i>	<i>X</i>	<i>X</i>	<i>Corallinaceae</i> ; <i>Gigartina skottsbergii</i> ; <i>Iridaea cordata</i> ; <i>Palmaria decipiens</i> ; <i>Plocamium cartilagineum</i>
<b>Jerosch</b> (data: 2016, analysed by Abele; unpublished)	<i>X</i>	-	<i>X</i>	<i>X</i>

### 3.2.2 Additional data

During the German-Argentinian research cooperation in PC plenty of data has been collected that may be used in this study. An overview is given by Neder et al. (2016). Used data sets are environmental predictors for macroalgae, which are already edited for BIOMOD modeling in context of the work done by Jerosch et al. (n.d.). Additionally, glacier lines published by Rückamp et al. (2011) are used to obtain new ice-free water areas in PC. Satellite images, coastline shapes and bathymetry serve for visualization purposes and georeferencing information.

## 3.3 Preparation of macroalgal data for modeling

Georeferenced transect data of macroalgae is not consistently available. Some information is provided either in form of analog maps, of transects with only one available coordinate pair or of analyses not linked with GPS-Coordinates yet. Modeling software requires data to be spatially referenced to link them with predictor rasters. Macroalgal data sets presented in Table 1, where single locations of species are not georeferenced, are 1993/1994 Klöser, 1994-1996 Quartino and 2016 Jerosch transects. For data processing, the software ArcGIS for Desktop 10.3.1 and the script language Python 2.7 is used.

### 3.3.1 1993/1994 Klöser et al. data

Klöser et al. (1996) presented a composition map of macroalgae species in PC, which is derived from 14 transects recorded by a camcorder. Two transects are published with macroalgae coverage analyzed in detail (No. 3 and 13).

The first step to get the data into GIS is to adjust the cropped images to a spatial reference system with distinctive control points along the coastline (georeferencing). Afterwards desired patterns are portrayed into point, line or polygon features (digitalization). The result of this process is presented in Figure 3 (Chapter 2.1).

In order to receive presence/absence points the two provided analyses are combined with the belonging transects. Based on the analysis, points are generated where species occur or not occur. This approach is visualized in Figure 9.

Other presence/absence points were extracted from the digitalized composition map. Primarily points located close to other transects are created, because accuracy is assumed to be highest there.

3

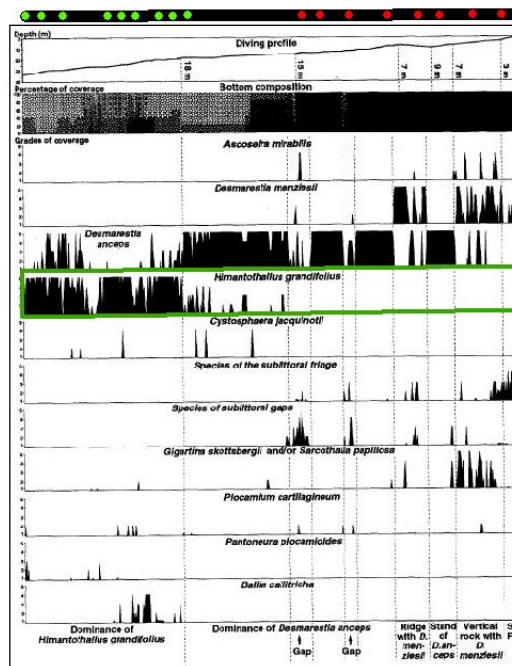


Figure 9: Coverage analysis (sheet with diving profile and observed species) combined with a georeferenced transect (black line labeled with a 3, referring transect No. 3). Green points represent digitalized presences, red points represent absences of *H. grandifolius* (observed species in green rectangle). Information received from Klöser et al. (1996).

### 3.3.2 1994-1996 Quartino and Boraso de Zaixso data

During the study of Quartino and Boraso de Zaixso (2007) biomass samples of six sites have been collected through scuba diving perpendicularly to the shore. Samples were taken at depths of 0, 5, 10, 20 and 30 m. One coordinate pair is given for each site in combination with the inherent depth of a sample point. Based on this information, points were relocated using depth contours. Figure 10 shows this process exemplary for one site.

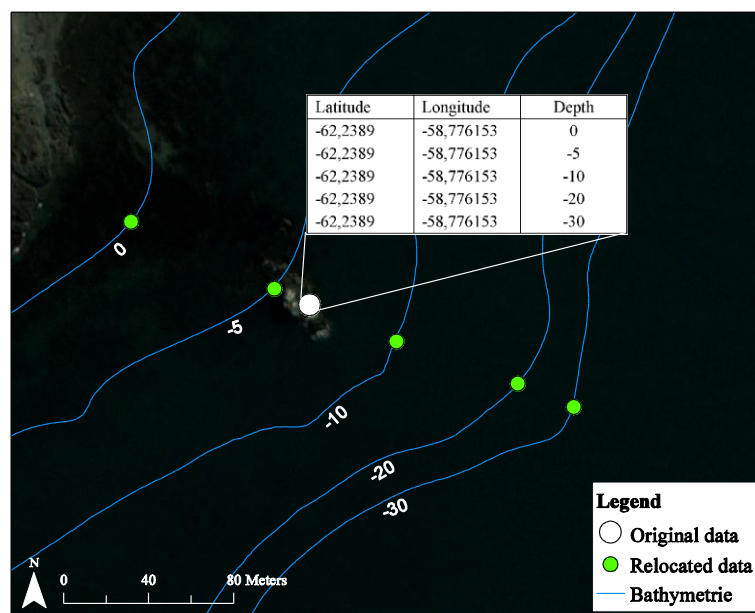


Figure 10: Relocated biomass samples along depth contours based on the original attribute table.

### 3.3.3 2016 Jerosch data

During the austral summer season 2015-16, K. Jerosch performed the latest georeferenced video data set distributed over most of the cove. Combined the lengths of analyzed transects exceed 10 kilometers. Recordings were taken by a SANYO HD Network SeaCam backed by a GoPro. The cameras were fixed to a TOV (towed operated vehicle), which was especially developed for this task by T. Gentz and K. Jerosch (both AWI). Towed by a motorboat, this vehicle is able to stabilize a few meters over the seabed, providing a good angle for the cameras to record the local ecosystem. Tracks of the boat were recorded by GPS sensors. Due to technical problems, multiple sensors were used, resulting in data with different time formats. With the software SANYO VMS Version 1.8.3 videos were analyzed and insights into the composition of the ecosystem were logged in an Excel sheet. Eight recording days were performed. All available SANYO HD material was analyzed by D. Abele (AWI). SANYO HD material of the 06.02.2016 is corrupted, hence GoPro videos are used for the analysis of this day. Table 2 gives an overview over used data.

Table 2: Recording days, time format of used GPS recorder and analyzer of the result videos.

Date	Time format	Analyzed by
18.01.2016	124340	D. Abele
23.01.2016	183316	D. Abele
27.01.2016	column day: 27.01.2016 column time: 12:03:01	D. Abele
06.02.2016	2016/02/06 20:43:14	L. Weber
10.02.2016	2016/02/10 11:53:38	D. Abele
17.02.2016	2016/02/17 17:15:33	D. Abele
24.02.2016	2016/02/24 15:55:28	D. Abele
05.03.2016	2016/03/05 15:43:03	D. Abele

During boat trips through the cove GPS recorders created a georeferenced point approximately every one to fifteen seconds. The video analysis tables consist of periods, where macroalgal community is similar. For these periods absence (0) or the quantity of species cover (1-3) is recorded together with community description and sediment structure. The structure of both tables is exemplary visualized in Tables 3 and 4.

Table 3: Extract of the GPS shapefile attribute table (18.01.2017).

Shape*	type	time	latitude	Longitude
Point ZM	TRACK	124902	-62,23779140	-58,66825417
Point ZM	TRACK	124908	-62,23779115	-58,66826490
Point ZM	TRACK	124920	-62,23779509	-58,66827697
Point ZM	TRACK	124934	-62,23780531	-58,66831133
Point ZM	TRACK	124935	-62,23780917	-58,66832240
Point ZM	TRACK	124939	-62,23781076	-58,66833162
Point ZM	TRACK	124944	-62,23782132	-58,66837964
Point ZM	TRACK	124954	-62,23783767	-58,66847050



Table 4: Extract of the Microsoft Excel video analysis table (18.01.2017)

time	community	sediment structure	Desmarest	Phaeo	Rhodo
12:43:15	camera preparation				
12:49:18	macroalgal fringe	sand and stones	1	0	2
12:53:28	macroalgal belt	boulders	1	2	3
12:54:56	no visibility				
12:57:07	macroalgal belts	boulders	1	2	3
12:57:28	macroalgal belt	rock	1	3	3

To obtain presence/absence data points, both tables have to be joined based on the time field. However, in this condition a join between the tables would be incomplete due to missing seconds in the GPS file. For example the start of macroalgal fringe at 12:49:18 (Table 4) could not be linked to an entry in Table 3. GPS points have to be available every second.

To accomplish that task an approach is developed, interpolating missing seconds with the related location. When working in projected coordinate systems (WGS 1984 UTM Zone 21S; EPSG: 32721), vector analysis may be applied for x and y point values. Figure 11 visualizes the approach of interpolating x-times depending on the number of missing seconds.

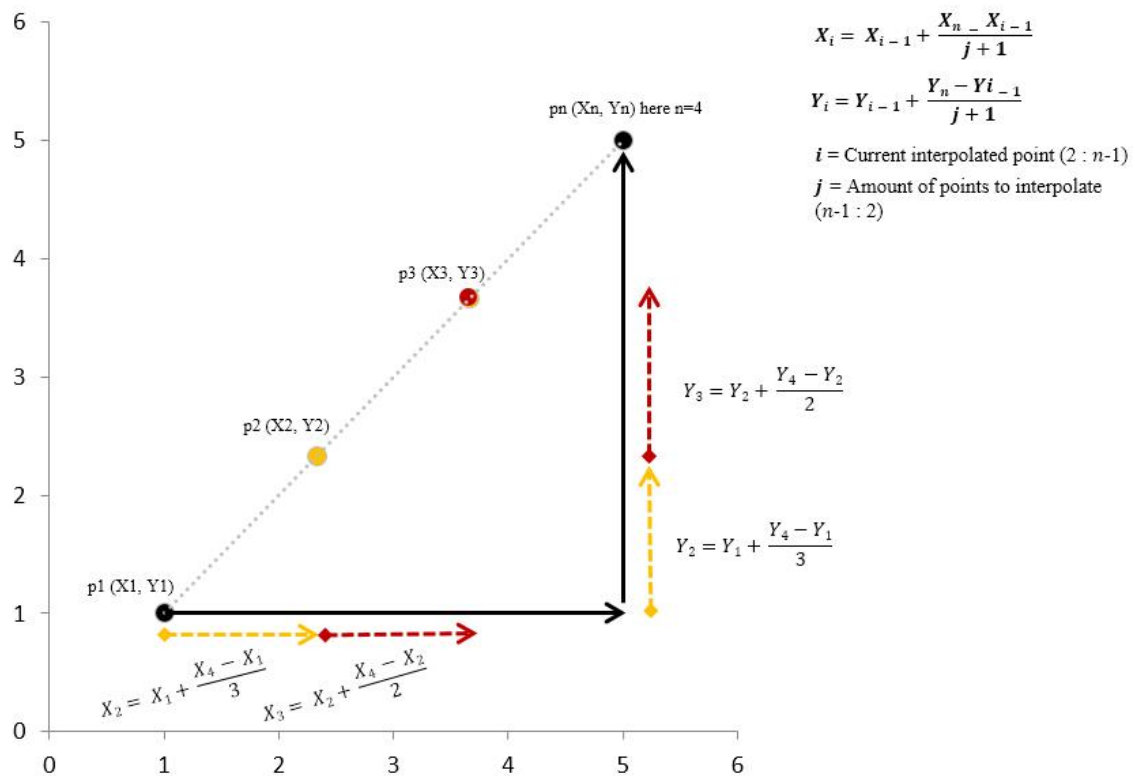


Figure 11: Interpolation of multiple points with constant gaps.  $p_1$  and  $p_n$  are given in the GPS file. Points in between are calculated by vector analysis. A general formula is necessary for the implementation of this method in a script.  $i$  iterates from 2 until the number of points to interpolate ( $n-1$ ).  $j$  iterates vice versa.



A Python script is developed to fill missing seconds in the GPS files and to join it with the video analysis table. The result file obtains a georeferenced point for every second of the video, along with the information whether a macroalgae species is present or absent. A simplified workflow of the script is visualized in Figure 12.

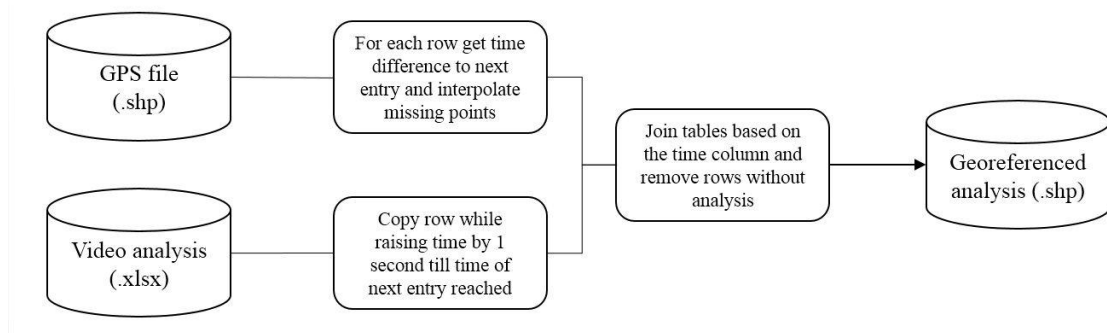


Figure 12: Workflow of combining video analysis tables with GPS files.

The script is reusable for every recording day, considering different time formats after retrieving the column with time information through a user dialog. All eight recording days are processed within this script, resulting in merged analyzed transects marked red in Figure 13.

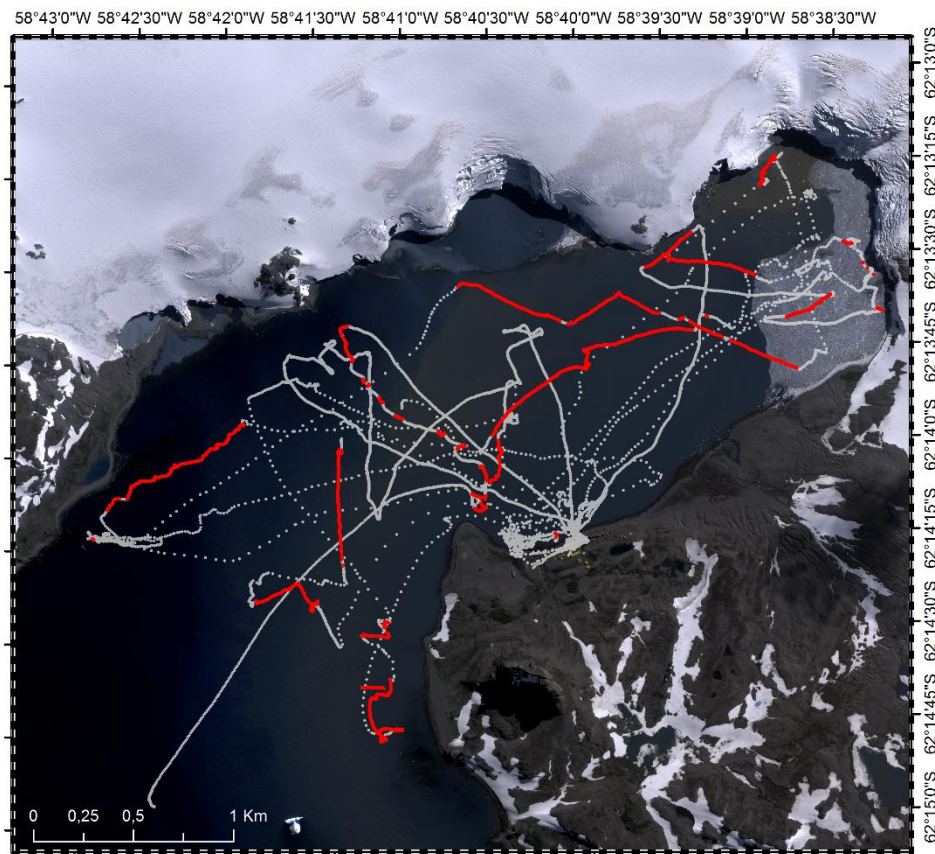


Figure 13: Analyzed video transects combined with GPS positions (red). Remaining tracks are visualized in grey and represent mostly travelling and bad view.

### 3.3.4 Grouping and merging macroalgal data into time steps

After preprocessing various macroalgal data to consistent spatially referenced data, six transect shapefiles are available for modeling. Since there is a clear temporal distinction between the 1993-1996 and 2008-2012 period, respective time steps will be grouped. 2016 data is available in a sufficient quantity to represent a third modeling subject. Transect groups and belonging sample types are presented in Table 5. The transect distribution of the respective time steps are visualized in Appendix 1.

Table 5: Grouping macroalgal transects into time steps for modeling. Coverage is the percentage of a picture/video covered by a species. Biomass is received by removing and weighting algae. Presence/Absence data sets represent points where a species was either observed or not. Grouped time steps are tagged with different colors.

Originator	Recording date	Sampling type
Klöser et al.	1993/1994	Coverage / Presence, Absence
Quartino and Boraso de Zaiuso	1994-1996	Biomass
Quartino et al.	2008	Coverage
Sahade et al.	2009	Coverage
Wölfl	2011/Jan 2012	Coverage
Jerosch	2016	Presence, Absence

Macroalgal samples are recorded in different types, thus grouped time steps are unified to 1 (presence) and 0 (absence). Presence will be applied for each algae species recorded with biomass or relative coverage greater than zero. The two former time steps are merged by a Python script considering type of sampling and individual macroalgal composition. Presence/absence is continuously available for *Desmarestia* genus, *H. grandifolius* species and the classes *Phaeophyceae* (without *Desmarestia* and *H. grandifolius*) and *Rhodophyceae*. 2016 *H. grandifolius* is ceasing because it was mixed up with *Ascoseira mirabilis* in the analysis and thus integrated in the *Phaeophyceae* class.

## 3.4 Modeling

For each time step distributions of each available macroalgal species/genus/class is modeled. The R package biomod2 (Thuiller et al. 2016) offers a compilation of commonly used modeling techniques and a subsequent model evaluation with the option to create an ensemble model computed by best performing single models (Thuiller et al. 2009). Therefore the statistical computer language R (R Core Team 2015) is used for modeling. A script used for macroalgae modeling by Jerosch et al. (n.d.), developed by H. Pehlke, F. K. Scharf and K. Jerosch (all AWI), is slightly amended and applied in this work. Species

distribution modeling process introduced in Chapter 2.2 is similar to BIOMOD modeling, yet model choosing is not required. Instead, different models are produced and evaluated, with the best single models exceeding a user defined threshold combined to an ensemble model. For more information regarding the modeling and evaluation process with BIOMOD please refer to Thuiller et al. (2009).

Considerable changes between this thesis to the macroalgae modeling process in PC described by Jerosch et al. (n.d.) are the emission of MaxEnt as modeling technique, the number of species input data sets, the number of permutations for evaluation of variable importance, various thresholds and less environmental predictors.

MaxEnt is a technique for presence only data (Elith et al. 2011). Because all data sets include various true absences which should be taken into consideration, this model is not utilized in this work. As Jerosch et al. (n.d.) modeled the totality of macroalgae in PC, one presence/absence data set was used for modeling. Now modeling should be applied on a species level as well as on multiple time steps, resulting in the 11 presence/absence data sets introduced in Chapter 3.3.4 (3 times *Desmarestia*, *H. grandifolius*, *Phaeophyceae*, *Rhodophyceae*; *H. grandifolius* missing in 2016). To reduce computational cost, the number of model runs is reduced from 20 to 2 and permutations to test the variable importance from 10 to 1. Total number of models is derived from number of model runs (2) times different model techniques (9) times species data sets (11), resulting in approx. 200 different models. It is not given that evaluation scores of model results exceed a fixed value, thus the threshold is adjusted manually for each species data set depending on the scores. Environmental predictors used for macroalgal distribution modeling in this study are: probability of hard substrate occurrence, SPM, bathymetry and slope. Each of these physical predictors are assumed to limit the environmental niche of macroalgae (Chapter 2.1). Biological or chemical predictors are not included in this thesis. For detailed description of the data sets please refer to Jerosch et al. (n.d.).

### 3.5 Community mapping

As presented in Chapter 2.2, community mapping may be performed using single species model results. The traditional way of receiving a community map is a cluster analysis with a subsequent statistical description of each class. Patterns in the single species model overlay may thereby be detected and described (Ferrier et al. 2002). In this thesis, however, a change detection should be applied on the three time step community maps. It cannot be assumed that maps are comparable after a cluster analysis. To achieve a comparability, a fixed classification pattern is developed, based on single species model probabilities. For each time step classes are created, based on the pattern visualized in Table 6. To perform this classification an R-script is developed using the packages “raster” (Hijmans 2015) and “rgdal” (Bivand et al. 2016) for raster processing.

Table 6: Community classification of a time step based on macroalgal modeling results. Percentages in the class definitions refer to the respective probability of occurrence.

Class number	Class name	Definition
0	Absence	No group above 50%
1	<i>Desmarestia</i>	<i>Desmarestia</i> group above 75%, all other groups below 50%
2	<i>Desmarestia</i> dominant	<i>Desmarestia</i> group above 75%, at least one other group above 50%
3	<i>H. grandifolius</i>	<i>H. grandifolius</i> above 75%, all other groups below 50%
4	<i>H. grandifolius</i> dominant	<i>H. grandifolius</i> above 75%, at least one other group above 50%
5	<i>Phaeophyceae</i>	<i>Phaeophyceae</i> group above 75%, all other groups below 50%
6	<i>Phaeophyceae</i> dominant	<i>Phaeophyceae</i> group above 75%, at least one other group above 50%
7	<i>Rhodophyceae</i>	<i>Rhodophyceae</i> group above 75%, all other groups below 50%
8	<i>Rhodophyceae</i> dominant	<i>Rhodophyceae</i> group above 75%, at least one other group above 50%
9	Mixed Community	Multiple groups above 75%
10	Single Appearances	One or more groups above 50%, but below 75%

### 3.6 Change detection

Chapter 2.3 states the possible application of change detection analysis on classified rasters using post-classification comparison methods. The “Image Difference” tool of ERDAS Imagine 2015 provides the calculation of change detection matrices between two rasters. The classified community maps are deployed as input data for this tool. Afterwards the resulting “from-to” information between different species may be analyzed to achieve insight into ecosystem changes. Additionally, areas with new macroalgal population may be identified and quantified. The aim of this thesis is primarily to compare possible areas of population growth with newly ice-free water areas.

### 3.7 Glacier retreat and newly ice-free water areas

Rückamp et al. (2011) visualized the retreat of Fourcade Glacier at KGI from 1956 till 2008. To receive quantitative information of released water areas, published historical glacier lines are clipped with the coastline. For each time step a polygon representing a newly ice-free water area is created and the respective area is measured. To continue the time series a Landsat scene recorded on 07. December 2016 is downloaded from the United States Geological Survey (USGS) EarthExplorer. The preparation of the downloaded data to a multispectral image of PC with a resolution of 15x15 meters is visualized in Figure 14. The resulting image is used to digitalize the actual glacier front and the ice-free water area between 2008 and 2016.

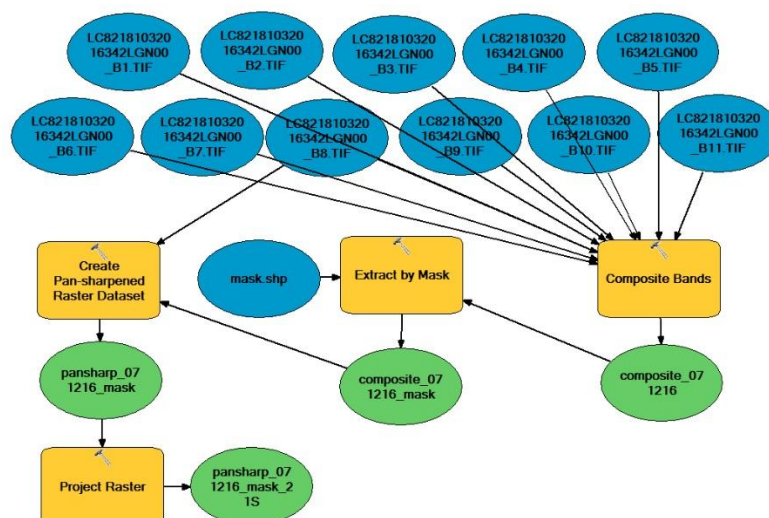


Figure 14: Workflow of processing a downloaded Landsat 8 scene. Created with ArcGIS ModelBuilder. Input data are 11 bands of a Landsat 8 scene.

## 4 Results and Discussion

### 4.1 Model results

This Chapter is separated into two parts, beginning with generic results regarding all models plus a comparison between them and followed by a detailed analysis of each particular time step.

After running the R script for all eleven data sets, following information for each group in each time step is obtained:

- **Projections** of the probability of occurrence; single models and ensemble model.
- **Response curves** of the models for every environmental parameter.
- Evaluation of **importance of environmental parameters** on modeling.
- Evaluation of **model performance**.

Overlapping model **projections** are visualized in Figure 15. To receive information on species richness and composition, these results are later classified into one raster, as described in Chapter 3.5. Following evaluation methods of model results are presented.

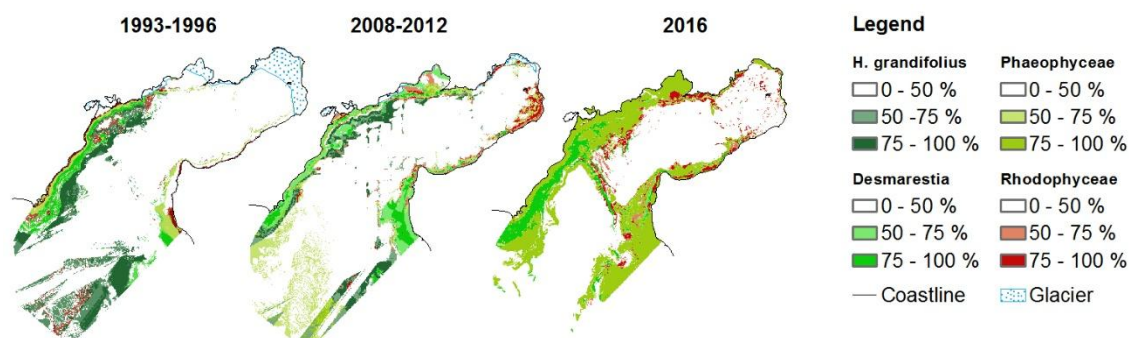


Figure 15: Overlapping model results of the respective time steps. Top layer is the first layer named in the legend, continuing in descending order. *H. grandifolius* is missing in 2016.

**Response curves** can provide insight into the environmental niche of a species (Guisan and Thuiller 2005). They visualize how a species model responds to various environmental predictors. An exemplary set of curves for the 1993-1996 *H. grandifolius* model is presented in Figure 16. Analysis of the **importance of environmental parameters** show that on average there is the most significant influence on species prediction at bathymetry with a factor of approx. 0.5. Hard substrate, SPM and slope follow with factors of approx. 0.3, 0.3 and 0.1.



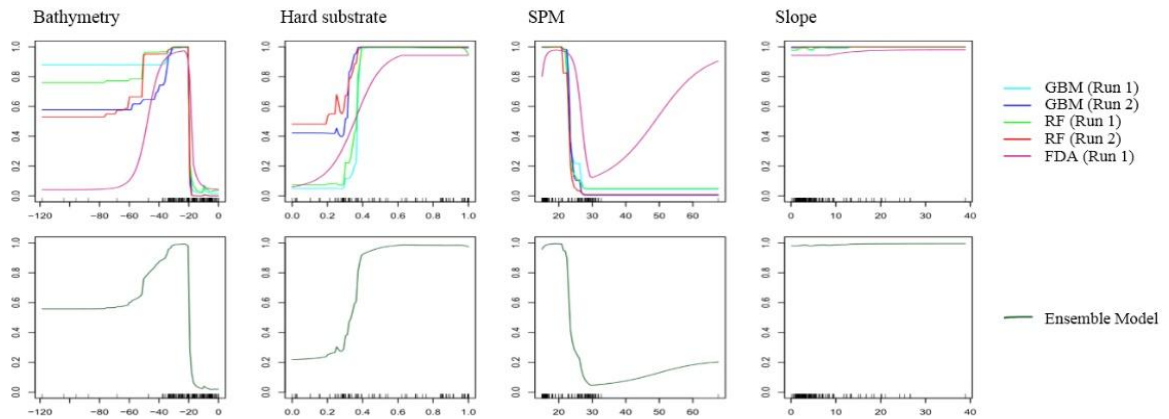


Figure 16: Response curves from both best single models and ensemble model.

In this case, *H. grandifolius* responds most on depths between 20 and 40 meters, a medium probability of hard substrate and lower SPM values. In order to evaluate model accuracy, response curves may be compared with ecological knowledge regarding the species. For this example the curves seem to be valid because all models have a similar response. All eleven models used in the following analysis and their corresponding response curves may be found in Appendix 2 and 3. Their TSS evaluation scores, which describes **model performances**, are visualized in Figure 17. According to Thuiller et al. (2010) TSS, which ranges from -1 to 1, defines “good” models with a score above 0.6. This is given in nearly every model.

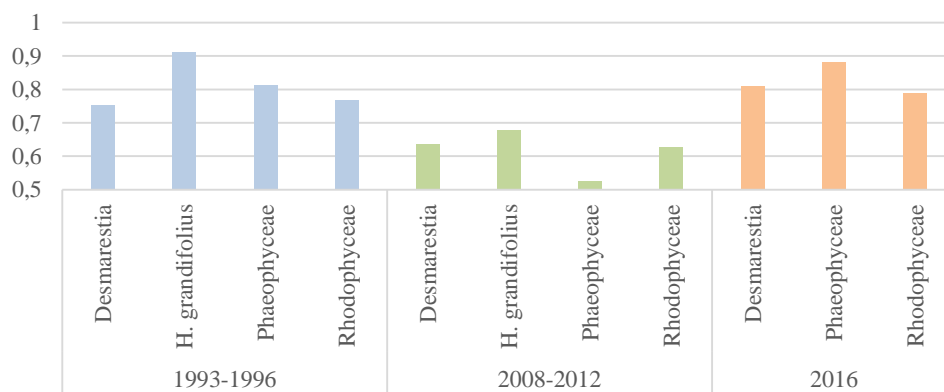


Figure 17: TSS evaluation scores of final models used in the following analyses.

Projections of models used in further analysis are the robust medians of best performing modeling approaches in BIOMOD. An exception are 2016 projections using only single models (see Chapter 4.1.3). The quantity of modeling approaches contributing to an ensemble model or being used as single model are visualized in Table 7. The four most used model algorithms are machine learning techniques confirming their success in species distribution modeling.

Table 7: Quantity of used BIOMOD modeling approaches

GBM	12
RF	9
ANN	8
CTA	7
FDA	6
GAM	4
GLM	3
MARS	2
SRE	0

The following subchapters describe the results of the respective time steps in detail.

#### 4.1.1 1993-1996

Model results regarding the 1993-1996 data set are the most suitable results. With the described methodology they have not only good TSS scores, but there also exist clear relations between visual comparison of the response curve and the presumed environmental habitat in PC. A relation is also apparent between presence/absence points and projections.

#### 4.1.2 2008-2012

Figure 17 shows that the 2008-2012 time step has generally a lower evaluation score. Multiple error sources must be mentioned. First, the data set is compiled by merging three different sources. Variations in sampling strategies and types may create imbalances during modeling. Second, hardly any samples are available at the coast of Potter Peninsula, limiting model accuracy in that part in comparison to 1993-1996 and 2016 data. And third, looking at the input species data sets, it is conspicuous that there is a large number of absence data covering some presences. This was considered during modeling process by giving less weight to absences than in other time steps. Nevertheless, studying over- and underprediction resulted in significantly more underpredictions (134 presence points under 50% probability) than overpredictions (53 absence points over 50% probability), using the *Desmarestia* data set as an example. It may be noted that 2008-2012 results are rather underpredicted. Additionally, their response curves do not fully fit to the known environmental habitat. For example *Phaeophyceae* and *Rhodophyceae* curves have peaks at high SPM values, which is assumed to limit macroalgal growth due to limited light availability. Thus, model results of the 2008-2012 time step must be viewed with a critical eye.

#### 4.1.3 2016

While 1993-1996 and 2008-2012 model projections are more or less satisfying due to visual comparison with presence/absence data, 2016 ensemble model results lack authenticity despite very good evaluation rates. Occurrence is predicted for far too deep areas where species are not expected to be able to live. Figure 18 depicts this exemplary on the ensemble model of *Rhodophyceae*, but this problem occurs in *Phaeophyceae* and partially in *Desmarestia* results, too.

Quite likely this problem occurs due to the conversion of high resolution video samples into modeling input data sets. Compared to satisfying 1993-1996 results where fewer points are rather well distributed, in 2016 lines of points every few decimeters are used as modeling input in 2016. Too many changes between presence and absence on a small



scale level may hamper model building, resulting in statistically most realistic habitats in bigger depths. A solution could be a reduction of the data sets' spatial resolution.

In order to still continue working on this study, response curves of single models are compared with each other and with the ensemble model. Information on environmental niches of the macroalgal species gathered from the ensemble model response curves of earlier time steps are used to find the most realistic 2016 single models. Artificial neural network (ANN) results for *Desmarestia* and *Phaeophyceae* as well as GAM results for *Rhodophyceae* promise the highest accuracy for further analyses.

Another issue for model quality are clear straight lines between predicted presence and absence, which are noticeable in most results. In Figure 18 this occurs in the outer cove at the lower left part of the image. These cuts are artefacts of the probability of hard substrate layer, which has been interpolated into the cove with few data points in this area.

Additionally the integration of *H. grandifolius* into the *Phaeophyceae* class leads to an implausible depth response curve in 2016. While two former time steps show a peak of *Phaeophyceae* probability in shallow depths, it is now dropping off in these areas. This is probably caused by the influence of *H. grandifolius*, which shows that response in former time steps. That must be taken into account while comparing *Phaeophyceae* results between the time steps.

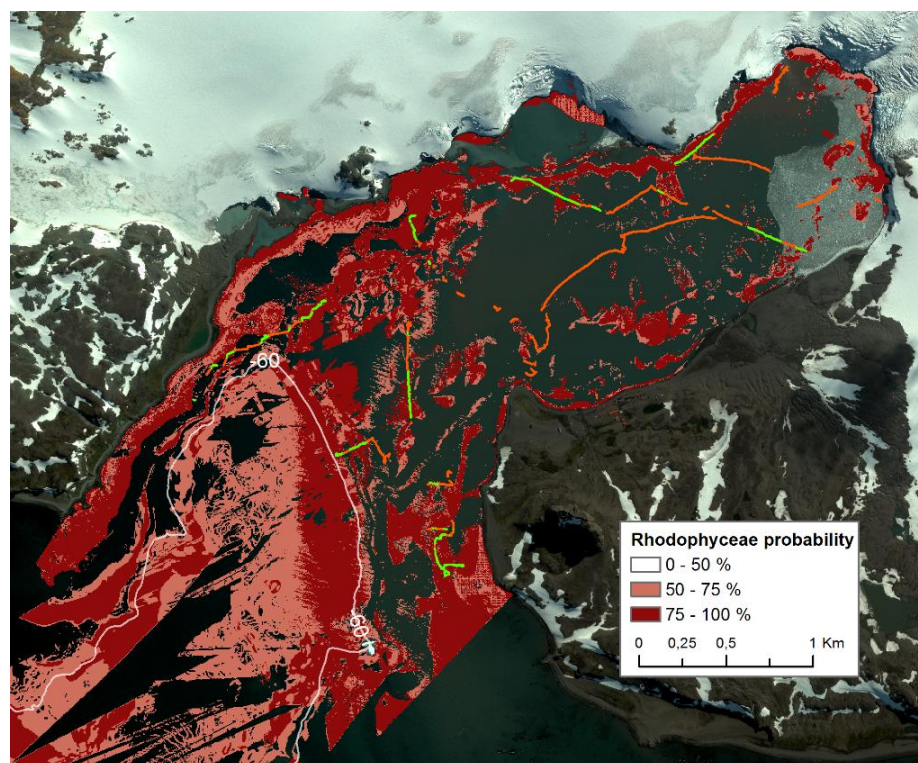


Figure 18: Ensemble model of 2016 Rhodophyceae class, including the used presence/absence points for modeling and the isobath of minus 60 meters.

## 4.2 Community maps

Through a concrete classification pattern a macroalgal community map is created for every single time step. Figure 19 presents the composed results, more detailed maps are arranged in Appendix 4. This Chapter describes and discusses the classification results and compares differences which are clearly recognizable. A numerical comparison between the macroalgal distributions ensues in the following Chapter.

Of particular note is that macroalgal communities in the outer cove are not as accurately classified as in the inner cove. Cuts are apparent, primarily in the 1993-1996 and 2008-2012 time steps, resulting from the hard substrate layer described in Chapter 4.1.3.

Another result, which is a consequence of the used classification pattern, is the high proportion of the “Mixed Community” class in 2016. Information on community composition gets lost in return for visual simplicity. It could be regained by comparing the class with single species maps or by raising the number of classes describing the composition of the mixed species. However, watching 2016 videos confirms at least partially that there is a big diversity between the species in narrow space. Thus, the high proportion of this class is accepted. There is a similar problem with the “Single Appearances” class. It is only visualized that there could be a macroalgal occurrence, but no further specification is provided.

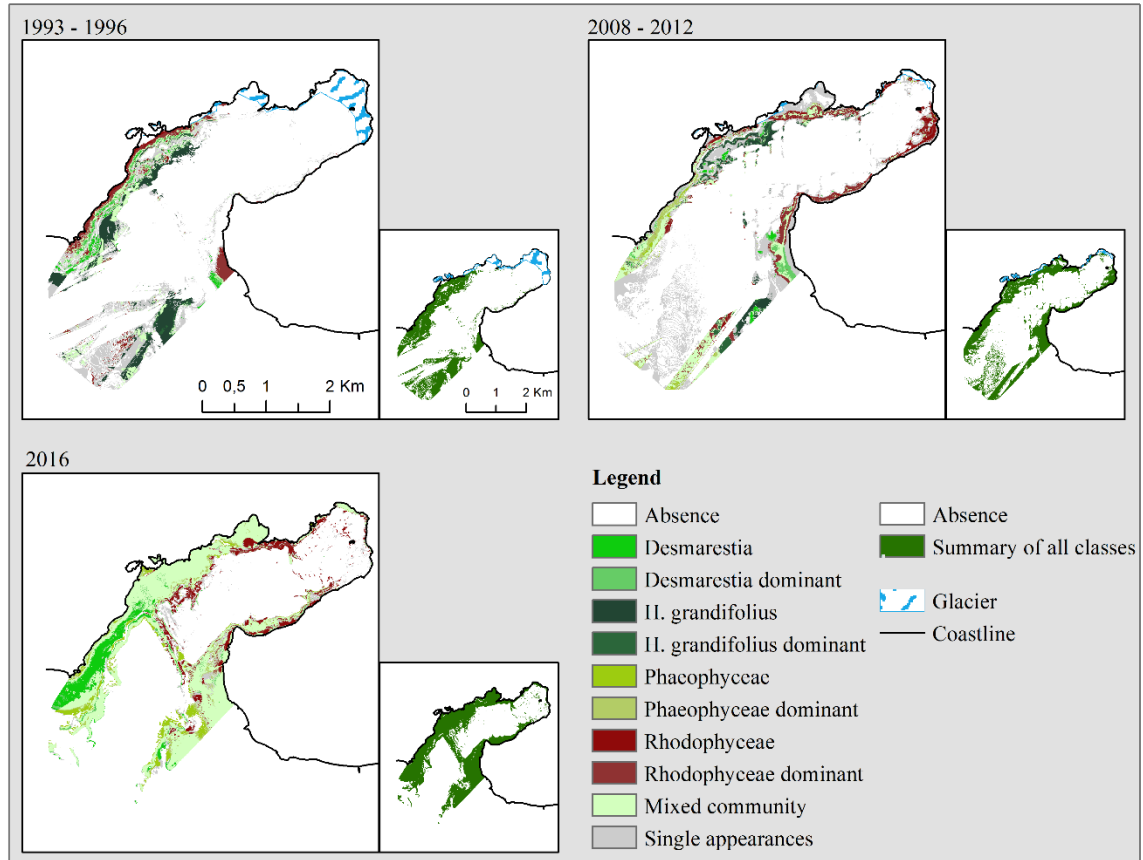


Figure 19: Community maps of the three time steps.

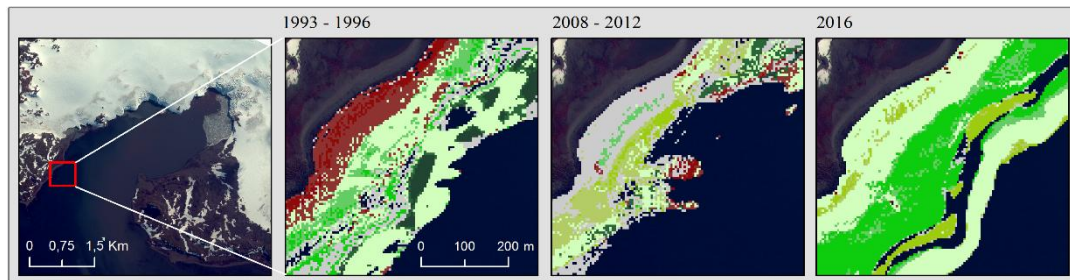


Figure 20: Small scale comparison of community maps in different time steps

This further complicates the principal aim of change detection, the description of changes between the single species. Figure 20 shows that too much connections exist among the time steps to be able to analyze in a framework of a bachelor thesis. Hence, the original concept is altered so that only the totality of macroalgal distribution is observed during change detection and not the species among each other. The totality of macroalgae in a time step is defined as all pixels in which at least one species has a probability of occurrence of 50 percent or more (visualized in smaller scaled maps of Figure 19).

Prior to moving on to change detection analysis an important finding should be noted before losing species information through generalization. In Figure 19 it becomes apparent that there is a shift of macroalgal distribution towards the glacier front. Both 2008-2012 and 2016 results validate that species of the class *Rhodophyceae* are pioneers in exploring new habitable areas. This is confirmed by a study of Quartino et al. (2013), where red algae *Palmaria decipiens* dominates in areas with high sediment load and low light availability near the glacier. How macroalgal communities shift in general and in connection with newly ice-free areas is analyzed in the following Chapters 4.3 and 4.4.

### 4.3 Changes in macroalgal population of PC

As stated in the previous Chapter, change detection between time steps is reduced to the totality of macroalgae. Therefore a change raster consists only of three different values: gain of macroalgal population, loss of macroalgal population and no change. By overlaying a change raster onto the generalized community map of the earlier time step, changes may be visualized ideally. Please note that all “errors” described in context of change detection are purely technology-oriented. Biological explanations have to be done by experts. Figure 21 presents changes detected in the two available periods.

Following findings may be gained by these results:

- Initially conspicuous are changes at the coast of Barton Peninsula. In the first period a massive loss of macroalgae is recorded, while nearly exactly this area seems to be repopulated in the second period. This effect probably result from the underprediction of 2008-2012 models described in Chapter 4.1.2. It may be assumed that this area is rather consistently populated across the whole period of study.

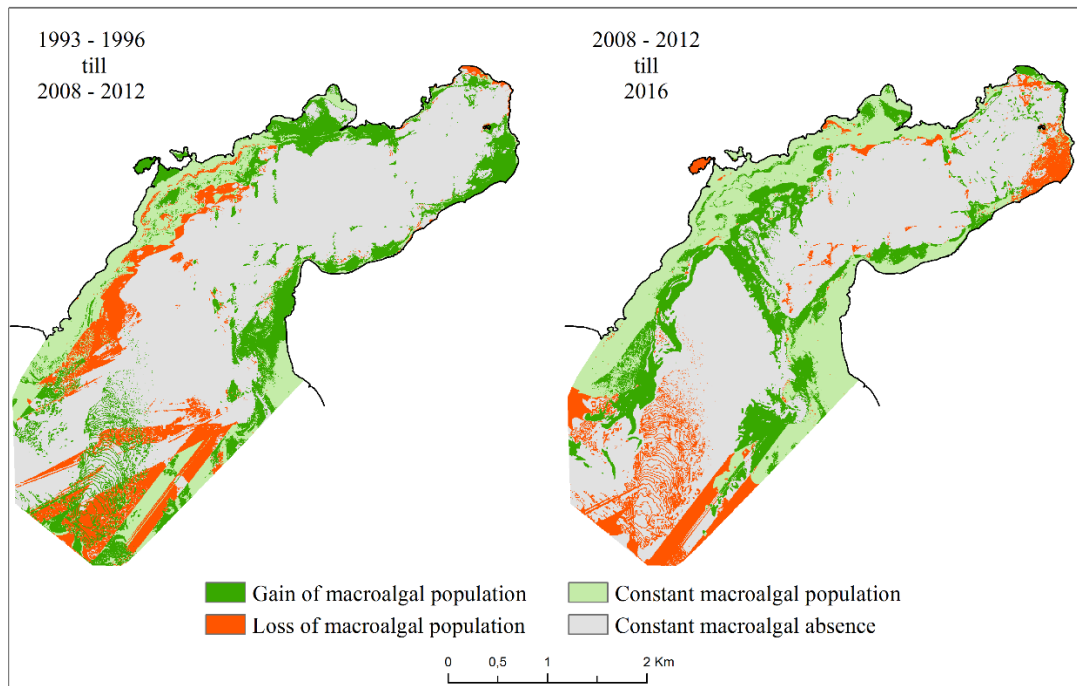


Figure 21: Change detection between the periods ~1993-2010 and ~2010-2016

- Open waters in the outer cove experience significant changes in both periods, caused by worse quality of environmental parameters than in the inner cove (see Chapter 4.1.3).
- The coast at Potter Peninsula experienced continual macroalgal growth during both periods. However, the most eastern part near the glacier, where 2008-2012 models predicted a big area of macroalgal population, is predicted free of algae for 2016. Video material confirms the second result. It is unlikely that there has been such a massive growth and an equal loss during ten years' time difference. Hence, 2008-2012 result is considered inaccurate for this area.
- The first glacier moraine (for location see Figure 8) is partly predicted to be populated by macroalgae in both earlier time steps, despite that no samples are available for this location. In 2016, where samples confirm algal occurrence on the moraine, it seems to provide a bridge between the two coastlines of the cove.
- It should be noted that Figure 21 does not include historical glacier areas. This is because these are subject to change within a period. A small section of both periods under the glacier may be treated as uninhabitable, which is examined closer in the following Chapter. Additionally at the most northeastern coast, where a gain of macroalgal population is recorded in the second period, a shadow appears in the satellite image representing SPM load caused by glacier cliffs. Due to that shadow models treat this area as free of SPM and suitable for macroalgae, which is obviously not correct in close proximity to the glacier.



The analysis benefits from two recent data sets (2008-2012 and 2016) which may be compared to historical data. Uncertainties in change detection, especially in the first period, may mostly be explained through comparison with the second period. Considering model quality described in Chapter 4.1, this confirms that the 2008-2012 time step is of less quality than both others. The main findings of this analysis are that approximately one kilometer of Barton Peninsula's and 2 kilometers of Potter Peninsula's coastline was newly populated by macroalgae between 1993-1996 and 2008-2012. The second period between 2008-2012 and 2016 confirms this to be the case and further experiences some smaller growth. Conspicuous for 2016 is the colonization of the whole first glacier moraine which is yet to be proven. Figure 22 visualizes the quantitative development of macroalgae during the studied period.

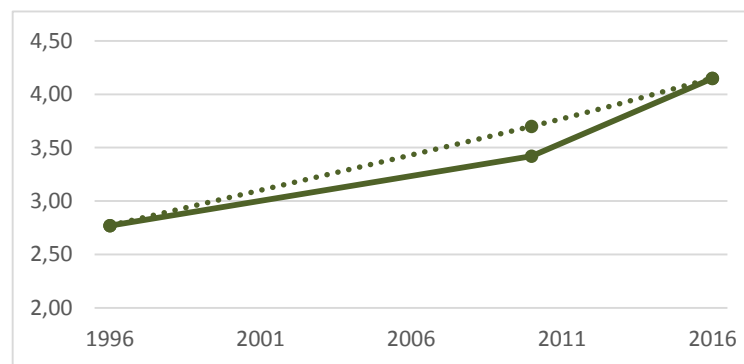


Figure 22: Area populated by macroalgae [km<sup>2</sup>]. The solid line indicates the original area figured out from model results. The dotted line represents the area assumed to be correct in 2008-2010 after the previous findings. For example the wrongly area loss at Barton Peninsula is added, the wrongly area gain near the glacier is subtracted.

The macroalgal population of PC rises from 2.77 km<sup>2</sup> in 1993-1996 to 4.15 km<sup>2</sup> in 2016. This corresponds to a gain of 1.38 km<sup>2</sup> within 23 years. 1993-1996 results are slightly overpredicted compared to a population area of 2.05 km<sup>2</sup> in Klöser et al. (1996). In order to receive this historical area, digitalized macroalgal shapefiles visualized in Figure 3 are clipped with the investigation area of this study. Reasons for overprediction may be the input of Quartino and Boraso de Zaixso data (1994-1996) as a second data set, inaccuracies in the models, especially in the outer cove, or digitalizing errors. Watching original result areas, the diagram indicates a significant increase of population after 2008-2012. Findings described one page before flowed into calculation of the dotted line, relativizing this increase. Nevertheless, the macroalgal colonization in PC remains on an upward trend since 1993-1996.

#### 4.4 Development of ice-covered water areas in PC in combination with macroalgal distribution shifts

The released water area from PC's Fourcade Glacier between 1956 and 2016 is visualized in Figure 23, partitioned in available time steps. Clearly most ice-cover back in 1956 melted, open water reaches the coastline almost everywhere. The quantitative progress of this decline confirms this to be the case. While 1956 1.5 km<sup>2</sup> of PC's water area was covered by ice, 2016 approximately 0,000175 km<sup>2</sup> are left. The process of glacier retreat accelerates between 1988 and 2000, before it slows down probably due to the proximity to the massive glacier at the mainland.

Figure 24 visualizes the comparison between newly ice-free water areas and macroalgal growth. 1996 macroalgal population just reached the historical glacier line of 1956. In the 20 years between 1996 and 2016 macroalgae populated 0.5 km<sup>2</sup> and therefore one third of newly ice-free area since 1956. However, a significant portion of this growth is located at a very flat (~50% < 1 meter depth) bay across from the research station. No samples are available in this area to prove macroalgal occurrence.

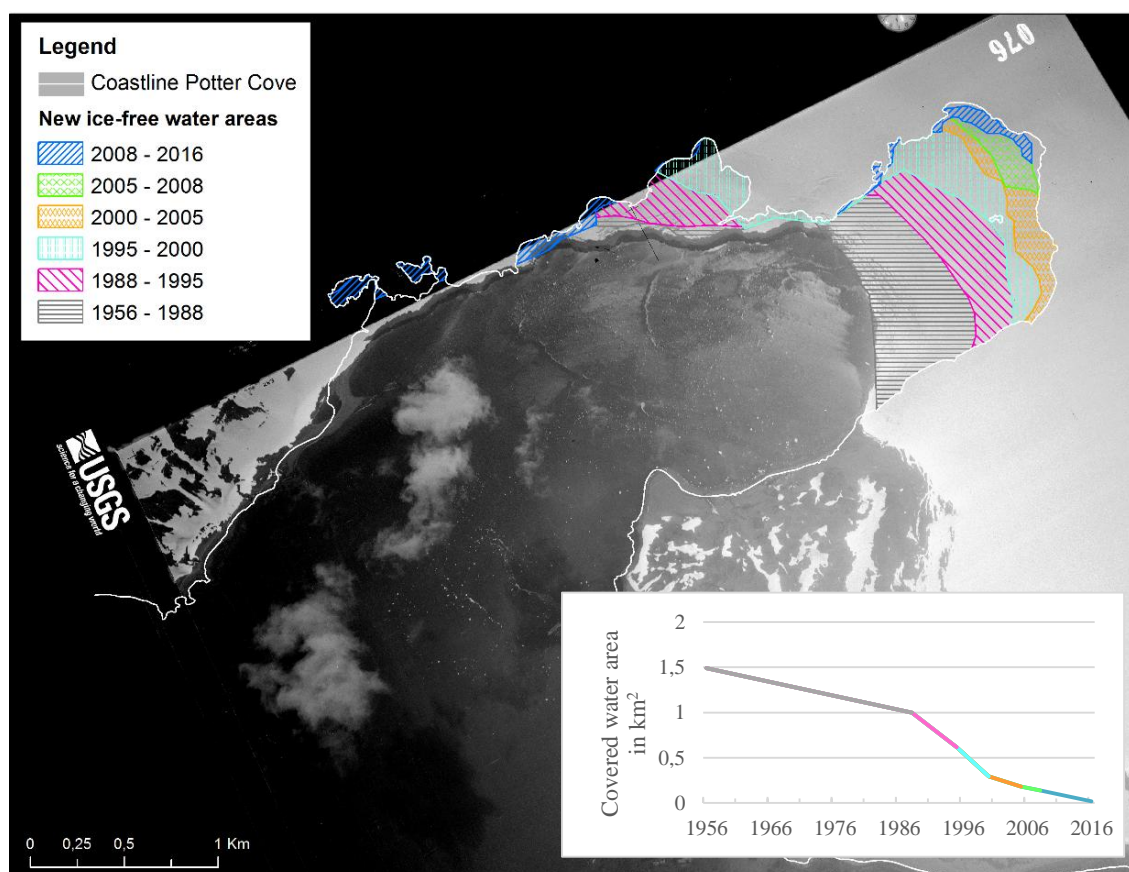


Figure 23: New ice-free water areas in PC due to glacier retreat. Colored are the ice-losses in the respective time step derived from Rückamp (2011) and a satellite image of 2016 (Chapter 3.7). Background image is an aerial photograph showing PC of 1956, downloaded from the USGS EarthExplorer. The diagram shows the quantitative loss of ice-covered water areas in PC [km<sup>2</sup>].

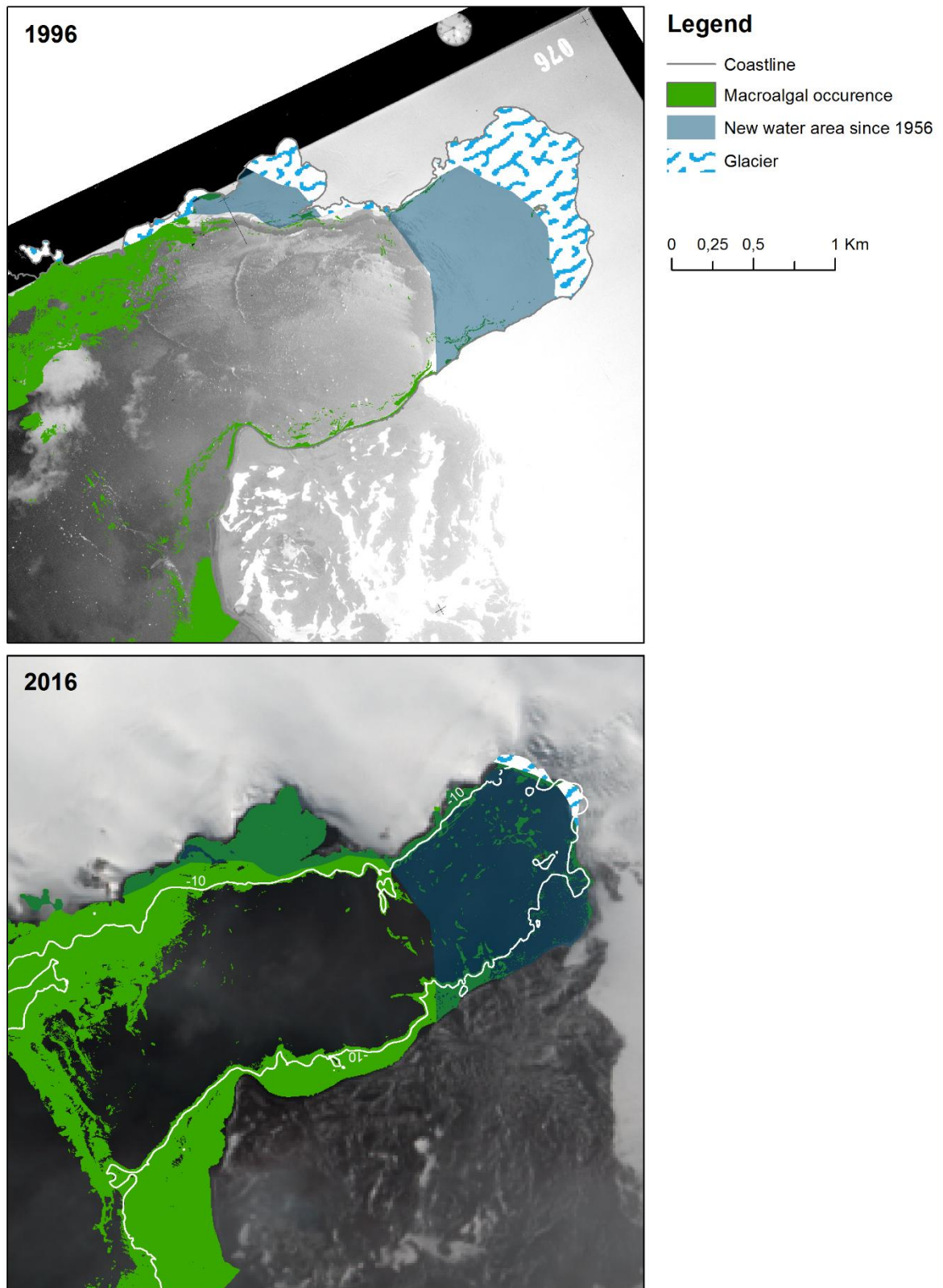


Figure 24: New ice-free water areas in PC compared with macroalgal population of 1996 and 2016. Background image are 1996 the aerial photograph of 1956 described in Figure 22 and 2016 the downloaded Landsat satellite image of 2016 described in Chapter 3.7. The color change of the newly ice-free water areas in 2016 is because the overlap with macroalgae population.

Macroalgae populating newly ice-free areas in 2016 are reduced in vertical distribution, very rarely exceeding a depth of 10 meters. This is caused by higher sediment input near the glacier, reducing light availability for photosynthesis (Quartino et al. 2013; Deregibus et al. 2015). In this study is shown that areas beyond the glacier 1956's line have a high proportion of "Mixed community". This can be confirmed with the statements of Chapter 4.2 that only some species are able to populate newly ice-free areas and Quartino et al.'s (2013, p3) finding that "the complexity of the macroalgal community is positively correlated to the elapsed time from the ice retreat".

#### **4.5 Future monitoring of macroalgae in PC**

The complete loss of glacier ice covering PC, which could happen before 2020, may mark a turning point in macroalgal colonization. No further new areas will be available for colonization, but sediment input from the glacier will continue due to melt water inputs (Falk et al. 2015), restricting deeper population of the seabed. Increase of macroalgal population visualized in Figure 22 has to flatten and stabilize at some time. Until then, monitoring of macroalgal colonization is important to gain insights into further adjustments of the ecosystem of PC to the occurred glacier retreat. The finding for improvement quality of this monitoring are presented in the previous chapters.

Multiple data set are available in PC (Neder et al. 2016). However, in this thesis, only physical parameters were used for BIOMOD modeling as environmental input data, excluding biological and chemical ones due a lack impact known for macroalgae. Marine biologist's expertise would be necessary to identify further valuable predictors. Video analysis of algae combined with GPS tracking provides a powerful way of sampling georeferenced high resolution data sets. Joining these information is possible using the Python script developed in this thesis. However, considering 2016 results, high spatial resolution should be reduced in the quantity of points. Meaningful and well distributed points seem to enable more robust models, which is the case in 1993-1996. Along with lower quality of 2016 video analysis, this indicates that the 2016 result could be considerably improved. Future monitoring of macroalgae in PC with SDMs and resulting community maps can be recommended. Sufficient predictors are available and models promise good results if mentioned factors are taken into account. New samples should still be taken along depth gradients perpendicular to the shore. Special points of interest concerning macroalgal population are the flat bay at Barton Peninsula as well as the first glacier moraine.



## 5 Conclusion

The questions tackled in this thesis are answered in the following:

- Is it possible to recreate historical community maps when analog historical species data is available?
- Is it possible to monitor shifts in macroalgal distribution using species data of multiple time steps? Which shifts can be described in PC?
- May these shifts be connected with the occurring glacier retreat in PC?
- Is the used methodology suitable for future monitoring of macroalgae?

Preprocessed point data sets with presence/absence information on species are grouped into the time steps 1993-1996, 2008-2012 and 2016. The macroalgal species/genus/class able to separate in this analysis are *H. grandifolius*, *Desmarestia*, *Phaeophyceae* (brown algae) and *Rhodophyceae* (red algae). Originating from those, single species models are created using SDMs. Subsequently the single results are classified in one community map for each time step.

As a result, three community maps can be presented. They hint information on the distribution and composition of macroalgae respectively for each time. Modeled 1993-1996 composition map provides a good representation of the digitalized input datasets as well as a quite homogenous comparison with the distribution map published by Klöser et al. (1996). The age of this data does not restrict model quality when predictors are constant in time. In this study, the historical data even ace two newer data sets in matter of model accuracy. 2008-2012 models are rather underpredicted and have lower evaluation scores while ensemble models of 2016 fail to comply the expected response curves. Anyway these models achieve the requirements for continuing the desired workflow.

Using post-classification comparison, a change detection method is deployed between the three time steps. The analysis resulted in macroalgal shifts, confirmed by both 2008-2012 and 2016 data. Stronger differences between the two newer maps can be reduced to inaccuracies of the model results. Due to the availability of two newer data sets for comparison the change detection can be assumed to be robust. Generally it can be mentioned that it is possible to monitor shifts in macroalgal distribution using species data of multiple time steps. Approximately one kilometer of Barton Peninsula's and two kilometers of Potter Peninsula's coastline are newly populated by macroalgae, primary not deeper than 10 meters. *Rhodophyceae* are the pioneers of this shift, while the community's complexity is reduced. These findings align with the latest research of Quartino et al. (2013) and Deregibus et al. (2015), analyzing macroalgal population in newly ice-free water areas.

Concerning glacier retreat it can be confirmed that newly ice-free water areas are colonized. One third of the newly ice-free area in PC since 1956 is populated by macrolage in 2016, 60 years later. However, it is difficult to provide a regularity or a formula of how fast newly ice-free areas are populated because in 1993-1996 macgroalgae have not reached the earliest known glacier line and the distribution in 2008-2012 and 2016 is quite similar.

---

Prospective studies can be realized using the described methodology. Chapter 4.5 states capabilities to improve model quality and to continue monitoring of macroalgae in PC in future. Further, information on the environmental niche of species received through modeling could be extrapolated to the whole coast of KGI or other parts of Antarctica. Field studies could review the validity and limits of such extrapolations. Species distribution modeling with subsequent community mapping is therefore an important tool to gather information on ecosystems in Antarctica and additional studies may build on the presented results.

## References

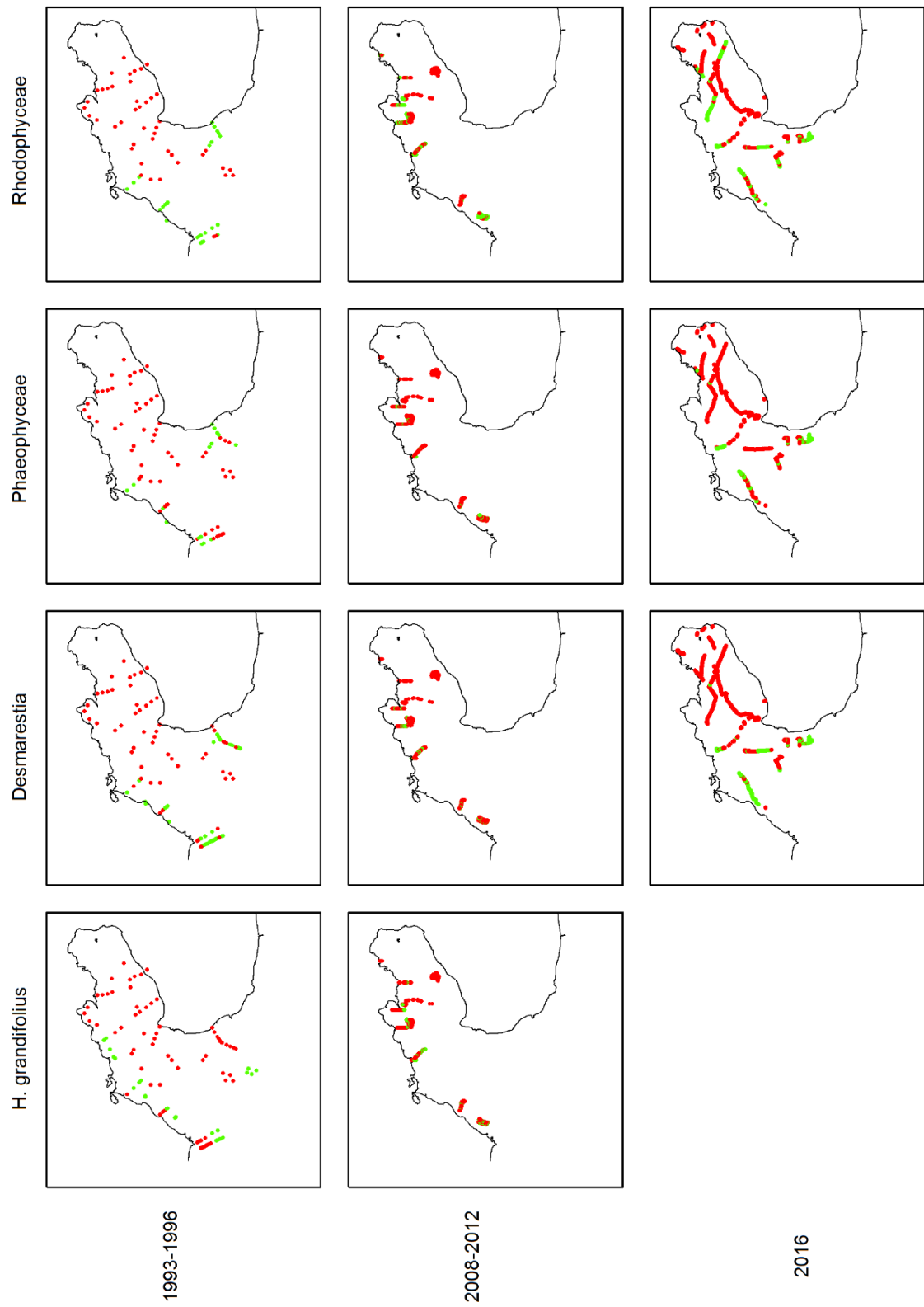
- Alphan, H., Doygun, H. and Unlukaplan, Y. I. 2009. 'Post-classification comparison of land cover using multitemporal Landsat and ASTER imagery: the case of Kahramanmaraş, Turkey', *Environ Monit Assess*, 151: 327-36.
- Araújo, M. B. and Guisan, A. 2006. 'Five (or so) challenges for species distribution modelling', *Journal of Biogeography*, 33: 1677-88.
- Barbet-Massin, M., Jiguet, F., Albert, C. H. and Thuiller, W. 2012. 'Selecting pseudo-absences for species distribution models: how, where and how many?', *Methods in Ecology and Evolution*, 3: 327-38.
- Becker, S., Quartino, M. L., Campana, G. L., Bucolo, P., Wiencke, C. and Bischof, K. 2011. 'The biology of an Antarctic rhodophyte, *Palmaria decipiens*: recent advances', *Antarctic Science*, 23: 419-30.
- Bivand, R., Keitt, T. and Rowlingson, B. . 2016. 'rgdal: Bindings for the Geospatial Data Abstraction Library. R package version 1.1-9. ', *rgdal package*, <http://cran.r-project.org/package=rgdal>.
- Brey, T., Voigt, M., Jenkins, K. and Ahn, I. 2011. 'The bivalve *Laternula elliptica* at King George Island — A biological recorder of climate forcing in the West Antarctic Peninsula region', *Journal of Marine Systems*, 88: 542-52.
- Brouwer, P.E.M. 1996. 'Decomposition in situ of the sublittoral Antarctic macroalga *Desmarestia anceps* Montagne', *Polar Biology*, 16: 129-37.
- Cawsey, E. M., Austin, M.P. and Baker, B. L. 2002. 'Regional vegetation mapping in Australia: a case study in the practical use of statistical modelling', *Biodiversity and Conservation*, 11: 2239–74.
- Clarke, A., Murphy, E. J., Meredith, M. P., King, J. C., Peck, L. S., Barnes, D. K. A. and Smith, R. C. 2007. 'Climate change and the marine ecosystem of the western Antarctic Peninsula', *Philosophical Transactions of the Royal Society B: Biological Sciences*, 362: 149-66.
- Cook, A. J., Fox, A. J., Vaughan, D. G. and Ferrigno, J. G. 2005. 'Retreating glacier fronts on the Antarctic Peninsula over the past half-century', *Science*, 308: 541-4.
- Coppin, P., Jonckheere, I., Nackaerts, K., Muys, B. and Lambin, E. 2004. 'Review Article Digital change detection methods in ecosystem monitoring: a review', *International Journal of Remote Sensing*, 25: 1565-96.
- Deregibus, D., Quartino, M. L., Campana, G. L., Momo, F. R., Wiencke, C. and Zacher, K. 2015. 'Photosynthetic light requirements and vertical distribution of macroalgae in newly ice-free areas in Potter Cove, South Shetland Islands, Antarctica', *Polar Biology*, 39: 153-66.
- DigitalGlobe. 2014. 'WorldView-2 scene 103001001F612100, Image Courtesy of / Copyright © DigitalGlobe - Longmont, Colorado. All rights reserved., Catalog ID: 103001001F612100, Acq Date: 2013/03/07, Sensor: WV02, Band Info: Pan\_MS1\_MS2, Resolution 0.5\*0.5m.'
- Dormann, C. F., Schymanski, S. J., Cabral, J., Chuine, I., Graham, C., Hartig, F., Kearney, M., Morin, X., Römermann, C., Schröder, B. and Singer, A. 2012. 'Correlation and process in species distribution models: bridging a dichotomy', *Journal of Biogeography*, 39: 2119-31.

- Elith, J. and Graham, C. H. 2009. 'Do they? How do they? WHY do they differ? On finding reasons for differing performances of species distribution models', *Ecography*, 32: 66-77.
- Elith, J. and Leathwick, J. R. 2009. 'Species Distribution Models: Ecological Explanation and Prediction Across Space and Time', *Annual Review of Ecology, Evolution, and Systematics*, 40: 677-97.
- Elith, J., Phillips, S. J., Hastie, T., Dudík, M., Chee, Y. E. and Yates, C. J. 2011. 'A statistical explanation of MaxEnt for ecologists', *Diversity and Distributions*, 17: 43-57.
- Falk, U., Gieseke, H., Kotzur, F. and Braun, M. 2015. 'Monitoring snow and ice surfaces on King George Island, Antarctic Peninsula, with high-resolution TerraSAR-X time series', *Antarctic Science*, 28: 135-49.
- Ferrier, S., Drielsma, M., Manion, G. and Watson, G. 2002. 'Extended statistical approaches to modelling spatial pattern in biodiversity in northeast New South Wales. II. Community-level modelling', *Biodiversity and Conservation*, 11: 2309–38.
- Gomez, I. and Huovinen, P. 2015. 'Lack of Physiological Depth Patterns in Conspecifics of Endemic Antarctic Brown Algae: A Trade-Off between UV Stress Tolerance and Shade Adaptation?', *PLoS One*, 10: e0134440.
- Guisan, A. and Thuiller, W. 2005. 'Predicting species distribution: offering more than simple habitat models', *Ecology Letters*, 8: 993-1009.
- Halpern, B. S., Walbridge, S., Selkoe, K. A., Kappel, C. V., Micheli, F., D'Agrosa, C., Bruno, J. F., Casey, K. S., Ebert, C., Fox, H. E., Fujita, R., Heinemann, D., Lenihan, H. S., Madin, E. M., Perry, M. T., Selig, E. R., Spalding, M., Steneck, R. and Watson, R. 2008. 'A global map of human impact on marine ecosystems', *Science*, 319: 948-52.
- Hijmans, R. J. 2015. 'raster: Geographic Data Analysis and Modeling. R package version 2.5-2.', *raster package*, <http://cran.r-project.org/package=raster>.
- Hijmans, R. J. and Elith, J. 2017. 'Species distribution modeling with R', *dismo-package*, <https://cran.r-project.org/web/packages/dismo/vignettes/sdm.pdf>: downloaded on 03.03.2017.
- Huang, Y. M., Amsler, M. O., McClintock, J. B., Amsler, C. D. and Baker, B. J. 2007. 'Patterns of gammaridean amphipod abundance and species composition associated with dominant subtidal macroalgae from the western Antarctic Peninsula', *Polar Biology*, 30: 1417-30.
- Iken, K., Amsler, C. D., Amsler, M. O., McClintock, J. B. and Baker, B. J. 2009. 'Field studies on deterrent properties of phlorotannins in Antarctic brown algae', *Botanica Marina*, 52.
- Jerosch, K., Scharf, F.K., Deregibus, D., Campana, G.I., Zacher, K., Pehlke, H., Falk, U., Hass, C., Quartino, M.L. and Abele, D. n.d. 'Habitat modelling as a predictive tool for analyzing spatial shifts in Antarctic benthic communities due to global climate change. ', (*in revision*).
- Klöser, H. and Arntz, W. E. 1995. 'RASCALS (Research on Antarctic Shallow Coastal and Litoral Systems) Untersuchungen zur Struktur und Dynamik eines antarktischen Küstenökosystems', *Polarforschung*, 64: 27-41.

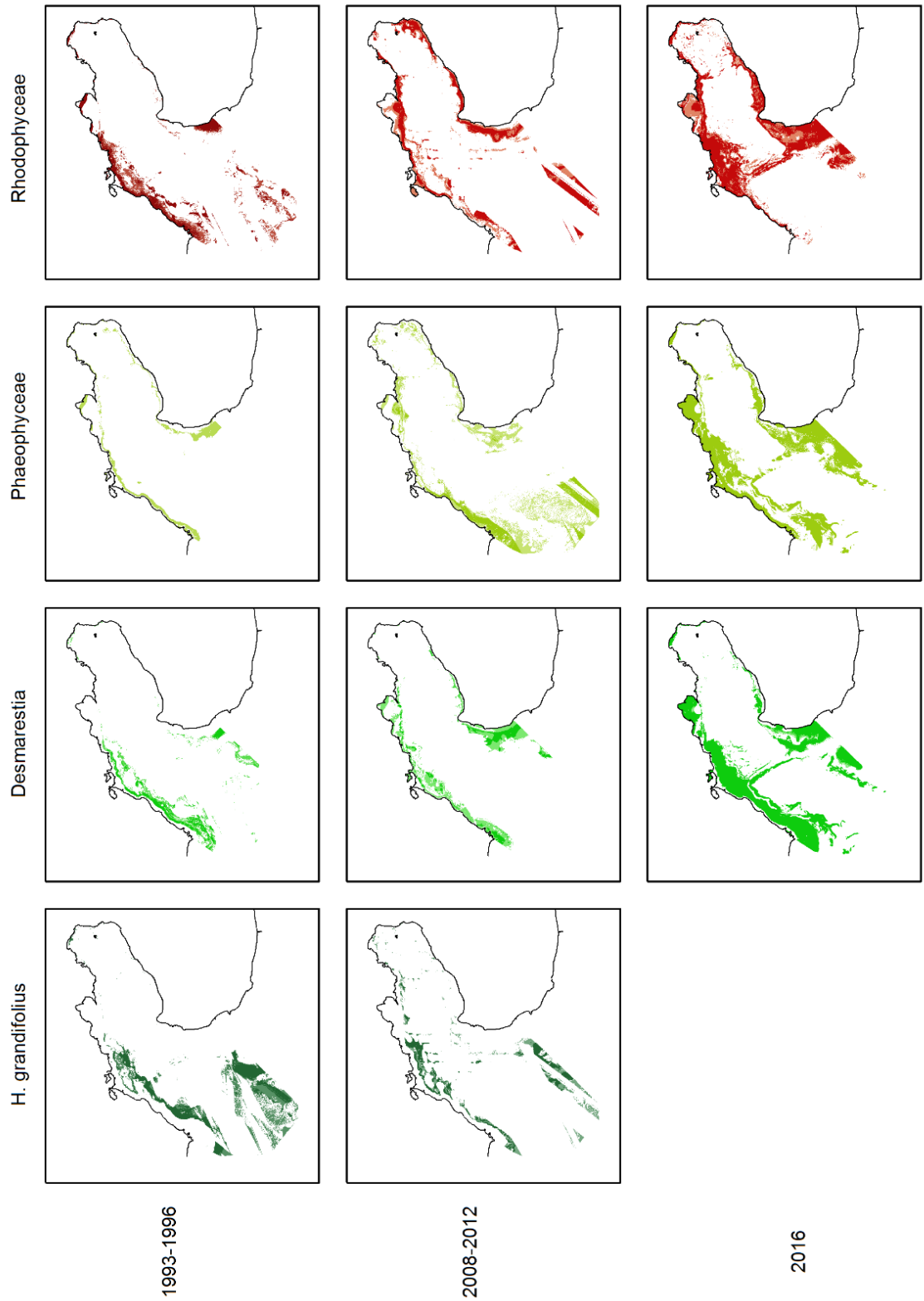
- Klöser, H., Ferreyra, G., Schloss, I., Mercuri, G., Laternus, F. and Curtosi, A. 1993. 'Seasonal variation of algal growth conditions in sheltered Antarctic bays: the example of Potter Cove (King George Island, South Shetlands)', *Journal of Marine Systems*, 4: 289-301.
- Klöser, H., Ferreyra, G., Schloss, I., Mercuri, G., Laternus, F. and Curtosi, A. 1994. 'Hydrography of Potter Cove, a Small Fjord-like Inlet on King George Island (South Shetlands)', *Estuarine, Coastal and Shelf Science*, 38: 523-37.
- Klöser, H., Quartino, M. L. and Wienke, C. 1996. 'Distribution of macroalgal communities in gradients of physical conditions in Potter Cove, King George Island, Antarctica', *Hydrobiologia*, 333: 1-17.
- Lenihan, J. M. 1993. 'Ecological response surfaces for North American boreal tree species and their use in forest classification', *Journal of Vegetation Science*, 4: 667-80.
- Lu, D., Mausel, P., Brondízio, E. and Moran, E. 2004. 'Change detection techniques', *International Journal of Remote Sensing*, 25: 2365-401.
- Marcías, M. L., Deregibus, D., Saravia, L. A., Campana, G. L. and Quartino, M. L. 2017. 'Life between tides: Spatial and temporal variations of an intertidal macroalgal community at Potter Peninsula, South Shetland Islands, Antarctica', *Estuarine, Coastal and Shelf Science*, 187: 193-203.
- Marmion, M., Parviainen, M., Luoto, M., Heikkinen, R. K. and Thuiller, W. 2009. 'Evaluation of consensus methods in predictive species distribution modelling', *Diversity and Distributions*, 15: 59-69.
- Mas, J.-F. 1999. 'Monitoring land-cover changes: a comparison of change detection techniques', *International Journal of Remote Sensing*, 20: 139-52.
- Morand, P. and Briand, X. 1996. 'Excessive Growth of Macroalgae: A Symptom of Environmental Disturbance', *Botanica Marina*, 39: 491-516.
- Neder, C., Jerosch, K. and Scharf, F. K. 2016. "What is available and who does it? Metadata available for German-Argentinian Cooperation compiled during IMCOAST/IMCONET Project: 25 Years of investigation in Potter Cove, Carlini Station, King George Island (Isla 25 de Mayo)." In.: PANGAEA.
- Philipp, E. ER, Husmann, G. and Abele, D. 2011. 'The impact of sediment deposition and iceberg scour on the Antarctic soft shell clam *Laternula elliptica* at King George Island, Antarctica', *Antarctic Science*, 23: 127-38.
- Pineda, E. and Lobo, J. M. 2009. 'Assessing the accuracy of species distribution models to predict amphibian species richness patterns', *J Anim Ecol*, 78: 182-90.
- Quartino, M. L. and Boraso de Zaixso, A. L. 2008. 'Summer macroalgal biomass in Potter Cove, South Shetland Islands, Antarctica: its production and flux to the ecosystem', *Polar Biology*, 31: 281-94.
- Quartino, M. L., Deregibus, D., Campana, G. L., Latorre, G. E. and Momo, F. R. 2013. 'Evidence of macroalgal colonization on newly ice-free areas following glacial retreat in Potter Cove (South Shetland Islands), Antarctica', *PLoS One*, 8: e58223.
- R Core Team. 2015. 'R: A language and environment for statistical computing. R Foundation for Statistical Computing, Vienna, Austria. ', <https://www.r-project.org/>.

- Radke, R. J., Andra, S., Al-Kofahi, O. and Roysam, B. 2005. 'Image change detection algorithms: a systematic survey', *IEEE Transactions on Image Processing*, 14: 294-307.
- Rückamp, M., Braun, M., Suckro, S. and Blindow, N. 2011. 'Observed glacial changes on the King George Island ice cap, Antarctica, in the last decade', *Global and Planetary Change*, 79: 99-109.
- Sahade, R., Lagger, C., Torre, L., Momo, F., Monien, P., Schloss, I., Barnes, D. K. A., Servetto, N., Tarantelli, T., Tatián, M., Zamboni, N. and Abele, D. 2015. 'Climate change and glacier retreat drive shifts in an Antarctic benthic ecosystem', *Science Advances*, 1: e1500050.
- Schloss, I. R., Abele, D., Moreau, S., Demers, S., Bers, A. V., González, O. and Ferreyra, G. A. 2012. 'Response of phytoplankton dynamics to 19-year (1991–2009) climate trends in Potter Cove (Antarctica)', *Journal of Marine Systems*, 92: 53-66.
- Schofield, O., Ducklow, H. W., Martinson, D. G., Meredith, M. P., Moline, M. A. and Fraser, W. R. 2010. 'How do polar marine ecosystems respond to rapid climate change?', *Science*, 328.5985: 1520-23.
- Thuiller, W., Georges, D., Engler, R. and Breiner, F. 2016. 'biomod2: Ensemble Platform for Species Distribution Modeling. R package version 3.3-7.', *biomod2 package*, <http://cran.r-project.org/package=biomod2>.
- Thuiller, W., Lafourcade, B. and Araújo, M. B. 2010. 'Presentation Manual for BIOMOD. La-boratoire d'écologie Alpine, University Joseph Fourier, 946 Grenoble'.
- Thuiller, W., Lafourcade, B., Engler, R. and Araújo, M. B. 2009. 'BIOMOD - a platform for ensemble forecasting of species distributions', *Ecography*, 32: 369-73.
- Torre, L., Tabares, P. C. C., Momo, F., Meyer, J. F. C. A. and Sahade, R. 2017. 'Climate change effects on Antarctic benthos: a spatially explicit model approach', *Climatic Change*, 141: 733-46.
- Vaughan, D. G., Marshall, G. J., Connolley, W. M., Parkinson, C., Mulvaney, R., Hodgson, D. A., King, J. C., Pudsey, C. J and Turner, J. 2003. 'Recent rapid regional climate warming on the Antarctic Peninsula', *Climatic Change*, 60: 243-74.
- Wiencke, C. and Amsler, C. D. 2012. 'Seaweeds and their communities in polar regions', *Seaweed Biology*, Springer Berlin Heidelberg: 265-91.
- Wiencke, C., Ferreyra, G., Arntz, W. and Rinaldi, C. 1998. 'The Potter Cove coastal ecosystem, Antarctica : synopsis of research performed within the frame of the Argentinean - German cooperation at the Dallmann Laboratory and Jubany Station (King George Island, Antarctica, 1991-1997)', *Berichte zur Polarforschung (Reports on Polar Research)*, Bremerhaven, Alfred Wegener Institute for Polar and Marine Research, 299: 326 p..
- Wölfl, A.-C., Wittenberg, N., Feldens, P., Hass, H. C., Betzler, C. and Kuhn, G. 2016. 'Submarine landforms related to glacier retreat in a shallow Antarctic fjord', *Antarctic Science*, 28: 475-86.
- Zacher, K., Roleda, M. Y., Wulff, A., Hanelt, D. and Wiencke, C. 2009. 'Responses of Antarctic Iridaea cordata (Rhodophyta) tetraspores exposed to ultraviolet radiation', *Phycological Research*, 57: 186-93.

## Appendix 1: Input species data sets

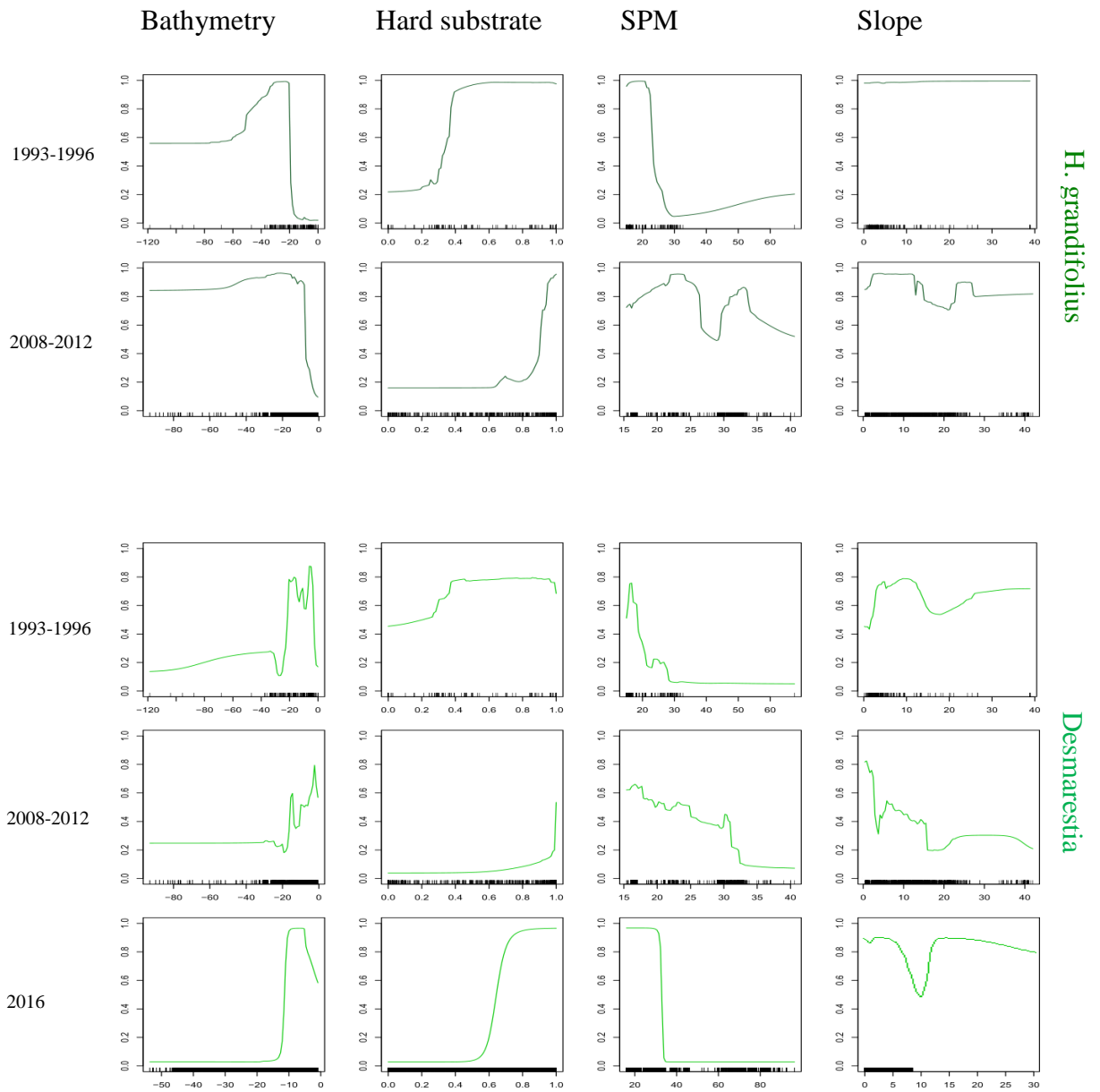


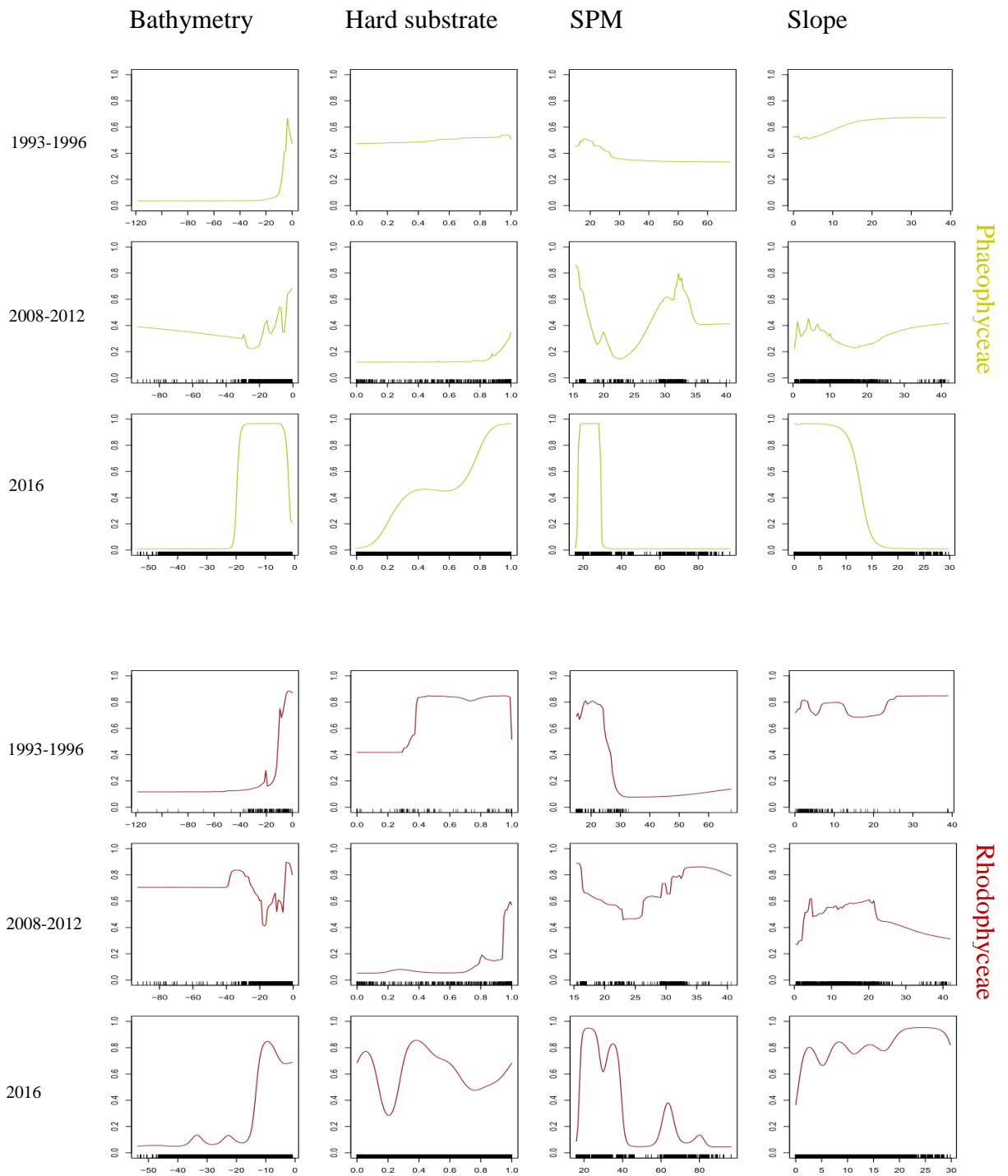
## Appendix 2: Model results





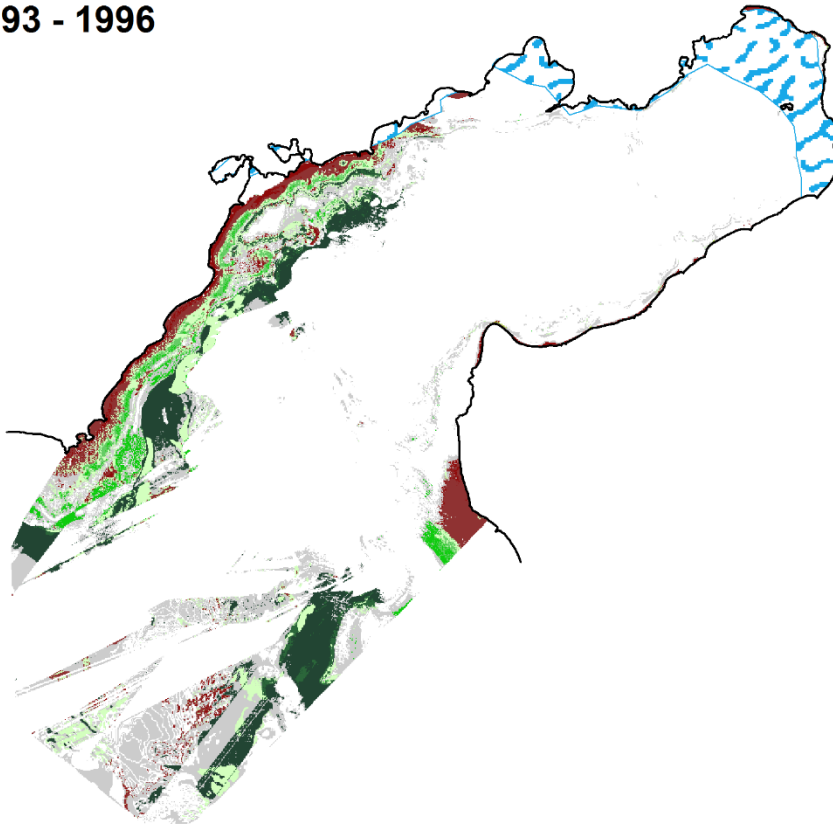
# Appendix 3: Response curves



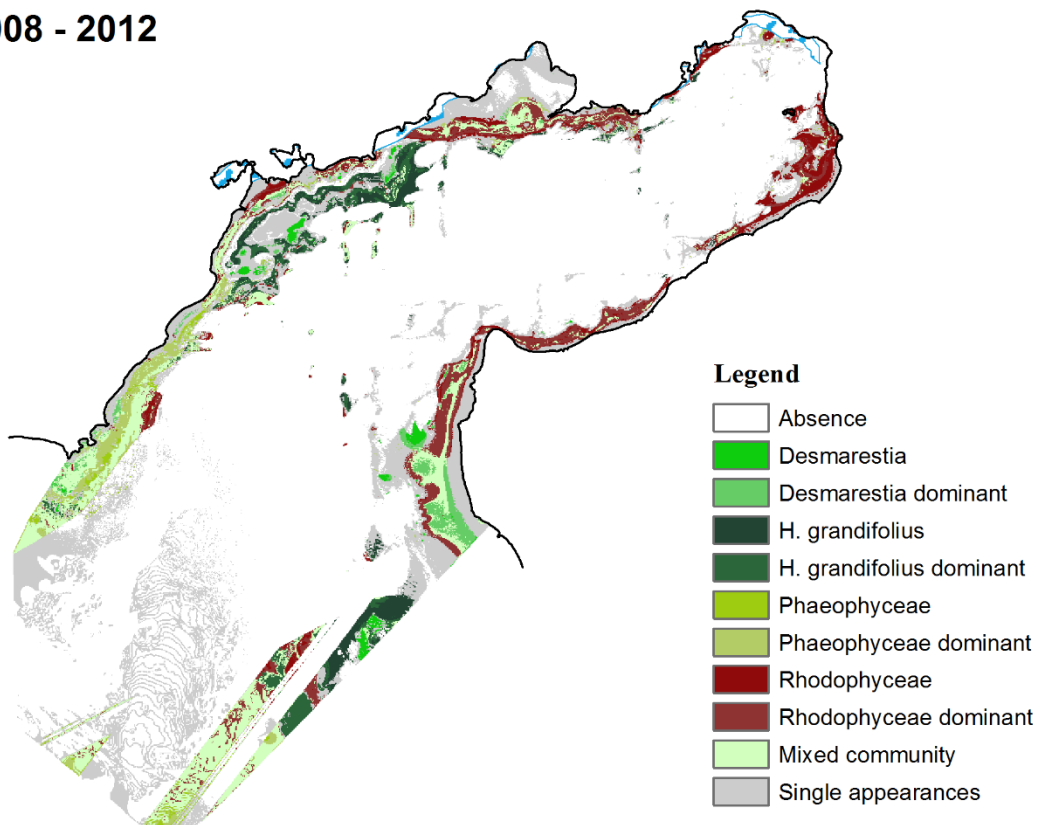


## Appendix 4: Community maps

1993 - 1996



2008 - 2012



2016

